Chapter One

Introduction

1 Introduction

Polypropionates form a class of structurally-diverse and biologically-significant molecules. Studies of their syntheses de novo and in vitro have afforded important insights into their structures and have led to the discovery and development of new synthetic methodologies.

1.1 Marine polypropionates

Over the past 30 to 40 years, an extensive list of structurally-diverse and biologically significant novel compounds has been isolated from marine organisms, such as bacteria and sponges.[1,2] A number of the metabolites isolated from these organisms have been shown to be biologically active and the main types of biological activity exhibited by these compounds can be divided into two categories:[1]

(i) cytotoxic - possess activity against cancer cell lines (most of the compounds currently undergoing clinical trials belong to this class)
(ii) anti-viral, anti-inflammatory, anti-coagulant and anti-parasitic

Out of those compounds that possess biological activity, only a very small number have survived the long road to be marketed as a human or veterinary drug. Their low isolation yields, in the order of milligrams of compound per kilograms of organism extracted, often require that the compounds be synthesised in the laboratory before they can be used for pharmaceutical development. However, the inherent complexity of the compounds makes synthesis difficult to achieve on a scale conducive to pharmaceutical application. Despite (and perhaps because of) their complexity, these structures have driven numerous synthetic efforts towards their synthesis. These endeavours have allowed a number of properties of the compounds to be elucidated, including their absolute stereochemistry. Further, they have progressed the development of existing synthetic methodologies available to organic chemists through discoveries of new reactions, as well as new applications of reactions already known in the literature.

One of the most important marine sources of these biologically-significant molecules are the Mollusca[2] and the majority of these compounds are related biosynthetically and structurally by the use of propionate units **1** as biosynthetic building blocks (Figure 1.1). Two examples of polypropionates isolated from molluscs (denticulatin A (**2**)[3] and siphonarin B (**3**))[4] are also shown in Figure 1.1.

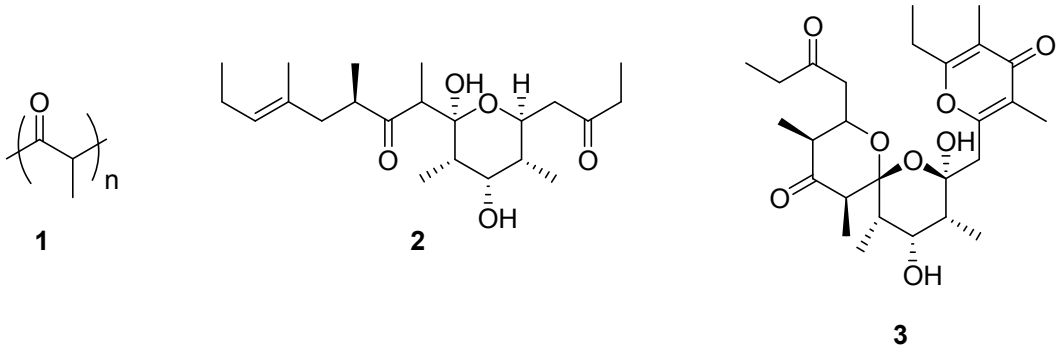

*Figure 1.1. The polypropionate building block **1**, denticulatin A (**2**) and siphonarin B (**3**).*

The condensation of propionate units **1** (Figure 1.1) leads to the characteristic array of structural features associated with polypropionates, which include alternating oxygenated and methylated carbon centres, multiple contiguous stereocentres and varying levels of unsaturation and oxidation, as exhibited by **2** and **3**.

The use of propionate units as building blocks for these structurally-complex molecules has been verified by extensive studies conducted on molluscs of the order Sacoglossa.[5-7] Biomimetic studies of the metabolites isolated from this family of molluscs have also yielded some interesting insights into the biosynthesis of these polypropionate compounds.

1.2 Marine sources of polypropionates

1.2.1 Sacoglossan molluscs

Molluscs of the order Sacoglossa play an important role in the ecology of benthic organisms and belong to a subclass of molluscs called Opisthobranchia.

Sacoglossans display the complete evolutionary series from shelled (which possess either a large or reduced shell) to shell-less molluscs (Figure 1.2) and are predominantly herbivorous, feeding in a suctorial manner on sponges, algae, soft corals and sea worms.[8] The lack of shell in some sacoglossan molluscs is compensated by the use of chemical secretions, nematocyst-based defences or cryptic coloration.[9]

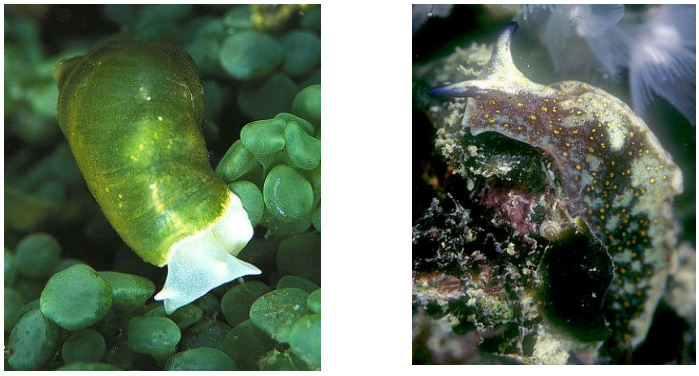

(a) (b)

Figure 1.2. (a) Shelled sacoglossan Volvatella viridis;[10] (b) shell-less sacoglossan Elysia japonica.[11]

Interestingly, sacoglossans are also able to retain live chloroplasts (kleptoplasty) from algal cells, which they obtain by piercing the algal cell wall with a specialized tooth.[9] The chloroplasts are utilised by the molluscs to produce secondary metabolites, including defence agents, which are especially useful in the case of shell-less sacoglossans. These defence agents possess cytotoxic, antimicrobial and feeding-deterrent activity towards micro-organisms, invertebrate eggs, sperm and larvae, marine fish and other molluscs.[9]

Studies on the feeding habits of sacoglossan molluscs have identified compounds that are accumulated from algae, such as sesquiterpenoid **4** and diterpenoid **5** (Figure 1.3)[8], which are in some instances chemically modified by the organism.

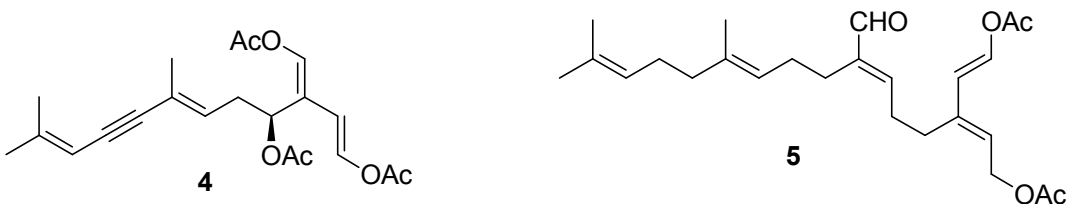

*Figure 1.3. Caulerpenyne (**4**) and udoteal (**5**).*[8]

Additionally, numerous compounds that are synthesised *de novo*, such as polypropionates, have also been isolated, with the Elysioidea superfamily of sacoglossan molluscs yielding an interesting array of polypropionate natural products.

1.2.2 Superfamily Elysioidea

True to their sacoglossan roots, molluscs of the superfamily Elysioidea also exhibit kelptoplasty and store the live chloroplasts in large parapodia, which contain branches of digestive glands (Figure 1.4).

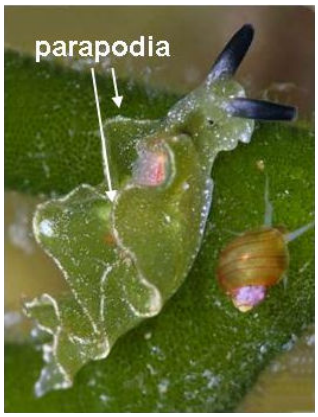

Figure 1.4. Elysia atroviridis with the two parapodia highlighted.[12]

The chloroplasts thus stored remain active for a few days, and are utilised to modify and synthesise compounds, particularly chemical defence agents.

In studies on five Mediterranean species of elysioideans (*Elysia translucens*, *Bosellia mimetica*, *Thuridilla hopei*, *Elysia timida* and *Elysia viridis*) it was found that *E. translucens*, *B. mimetica* and *T. hopei* bio-accumulated and bio-transformed

compounds (sesquiterpenoids and diterpenoids) from the algae that they consumed, while *E. timida* and *E. viridis* contained metabolites (polypropionates), which were absent in the dietary seaweeds.[8] It has been shown by ^{14}C-labelling experiments involving sacoglossan molluscs that the polypropionate metabolites isolated from these organisms are indeed synthesised *de novo* from propionate building blocks,[5] and a link has also been established between the photosynthetic activity of chloroplasts and the presence of polypropionate metabolites in the molluscs.[6,7] The extracts from mucous secretions of *E. timida* have also been shown to contain the same chemical profile as extracts of the animal itself,[6] which lends weight to the hypothesis that the polypropionate metabolites are part of the chemical defence system of sacoglossan molluscs, as discussed in Section 1.2.1.

Additionally, it has been found that the Mediterranean elysioideans share an almost identical chemical profile with their Pacific and Caribbean counterparts,[8] with Figure 1.5 showing the myriad of polypropionate metabolites, which have been isolated from elysioideans.[5,7,13-18]

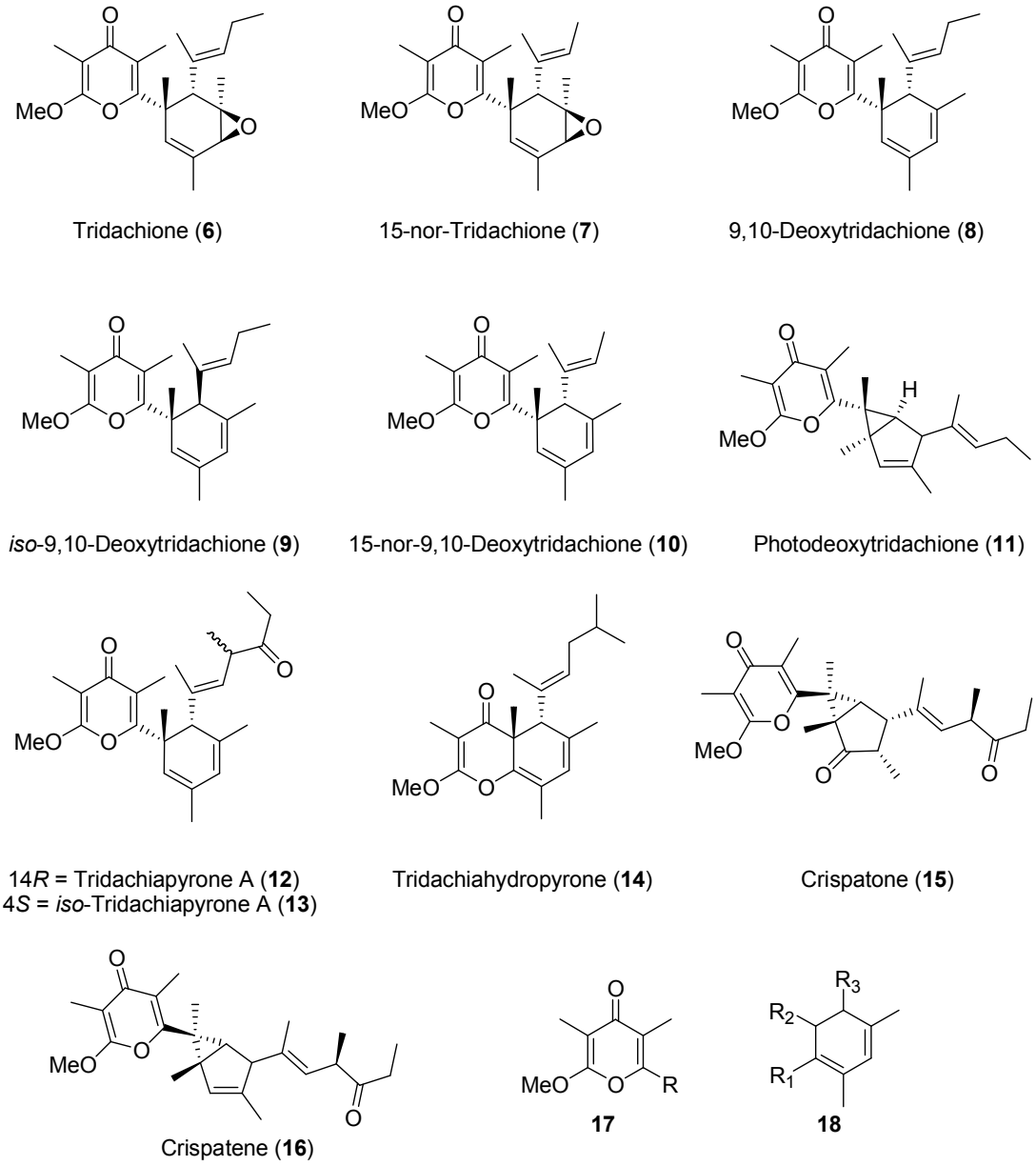

Figure 1.5. Reported structures of metabolites isolated from a variety of elysioidean molluscs.[5,7,13-18]

Due to the presence of both the γ-pyrone **17** and cyclohexadiene **18** motifs in many of the tridachiapyrones in Figure 1.5, it follows that any methodology developed towards the total synthesis of such compounds may provide novel pathways and access to the synthesis of other members of this large family of polypropionates. The synthesis of tridachiapyrones would allow their absolute stereochemistry to be determined (as only relative stereochemistry has thus far been reported) and would

provide potential avenues for the development of these compounds as therapeutic agents.

The discovery of the photo-catalysed conversion of 9,10-deoxytridachione (**8**) into photodeoxytridachione (**11**) by *Plachobranchus ocellatus* (Scheme 1.1), which also occurred in the laboratory in the presence of sunlight using benzene as the solvent,[7] has prompted a number of studies into this, and other photo-catalysed biomimetic processes, aimed at synthesising one or more of the γ-pyrone-containing polypropionates.

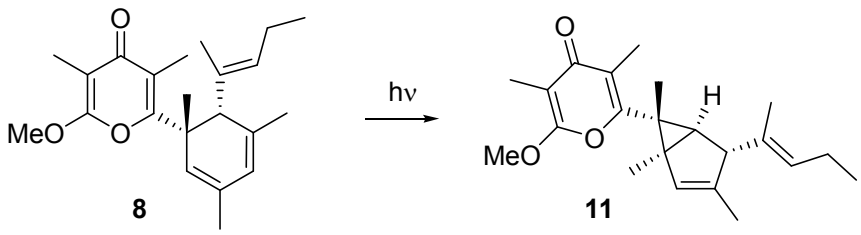

*Scheme 1.1. Photocatalysed conversion of 9,10-deoxytridachione (**8**) into photodeoxytridachione (**11**).*[7]

1.3 Biomimetic synthetic studies

While a number of different tridachiapyrones have been the focus of synthetic studies in the literature, only the studies towards 9,10-deoxytridachione (**8**) and tridachiahydropyrone (**14**) will be discussed herein.

1.3.1 Studies towards 9,10-deoxytridachione (8)

It is the isomeric relationship between the cyclohexadiene moiety of 9,10-deoxytridachione (**8**) and the bicyclo[3.1.0]hexene moiety of photodeoxytridachione (**11**) (Scheme 1.1, Section 1.2.2), that has sparked interest in their biomimetic relationship. Studies on these systems have attempted to mimic the non-enzymatic, *in vivo* conversion of 9,10-deoxytridachione (**8**) into photodeoxytridachione (**11**) in a laboratory setting, with the aim of developing an understanding of the conversion, and applying the knowledge to the synthesis of the two natural products **8** and **11**.

Investigations into this process have been performed by Miller and Trauner[19-22] and Moses *et al*,[19-21] among others.

During studies towards the synthesis of SNF4435C (**19**) and SNF4435D (**20**), Trauner and co-workers synthesised triene **21** as a precursor to the model system of **19** *via* a series of olefination reactions from aldehyde **22**. It was found that **21** was converted into cyclohexadiene **23** at room temperature (Scheme 1.2).[22]

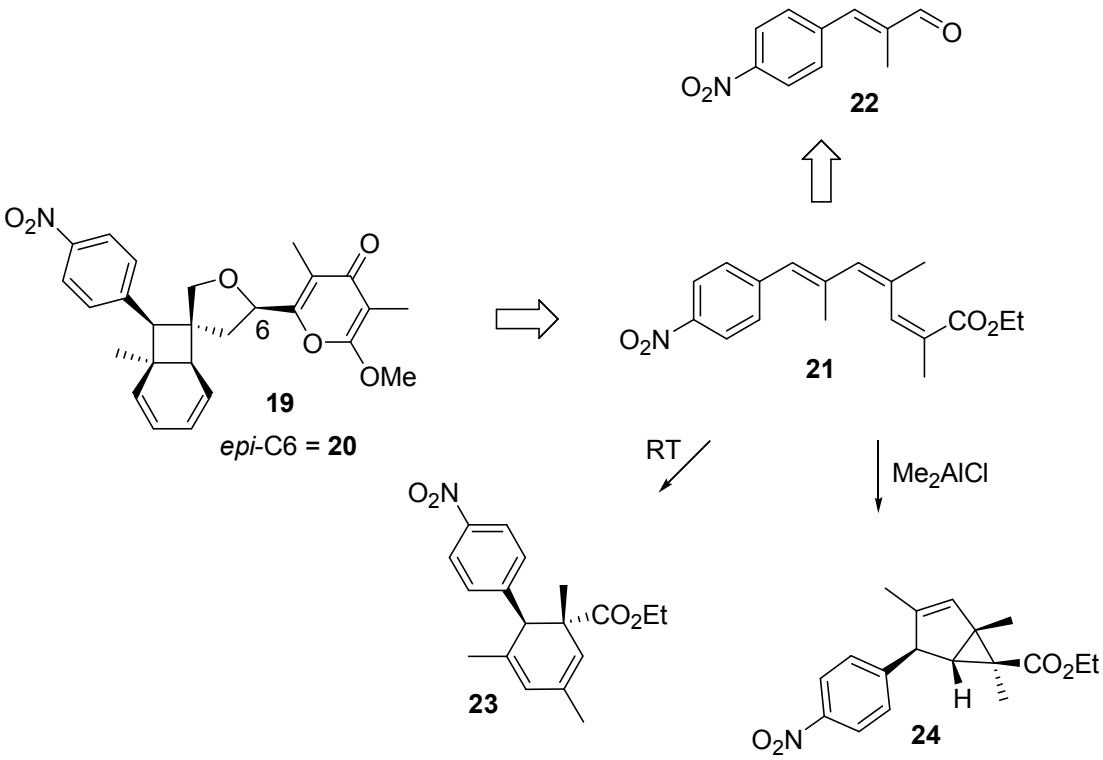

*Scheme 1.2. Observed conversion of triene **21** into cyclohexadiene **23** and bicyclohexene **24**.*[22]

In subsequent studies by Miller and Trauner into the use of polyenes as precursors to natural products, triene **21** was also converted to bicyclohexene **24** in the presence of a Lewis acid catalyst (Scheme 1.2).[23] This discovery led to application of the Lewis acid-mediated conversion to the total synthesis of (±)-photodeoxytridachione (**11**)[23] (Scheme 1.3), which was achieved from tetraene **25** (*via* bicyclohexene **26**).

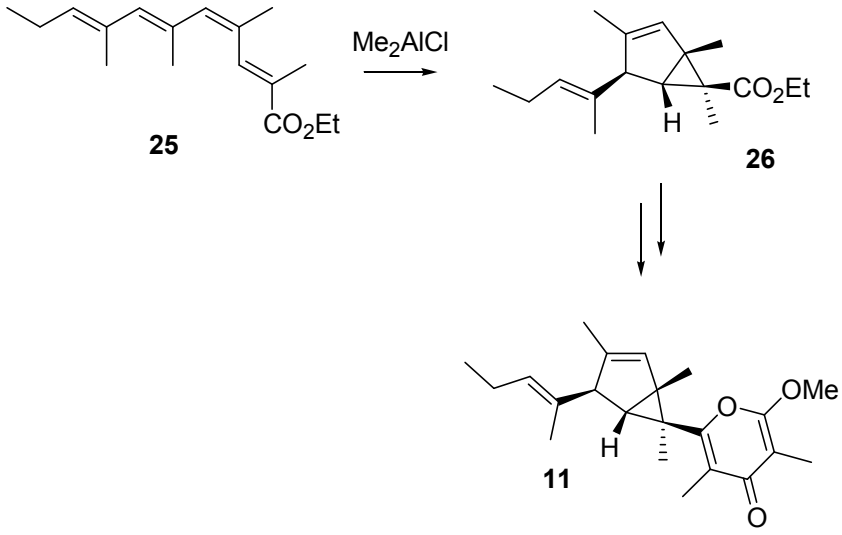

*Scheme 1.3. Conversion of tetraene **25** into bicyclohexene **26** in the total synthesis of (±)-photodeoxytridachione (**11**).*[23]

It was also found by Miller and Trauner that tetraene **27** converted to cyclohexadiene **28** and bicyclo[4.2.0]octadiene **29** when heated in benzene at reflux (Scheme 1.4).[24]

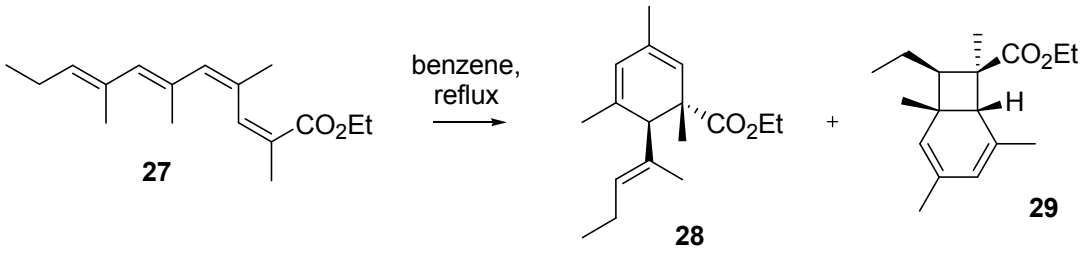

*Scheme 1.4. Formation of cyclohexadiene **28** and bicyclo[4.2.0]octadiene **29** from polyene **27**.*[24]

Based on the discoveries that triene **21** and tetraenes **25** and **27** are precursors to cyclohexadiene and bicyclohexene systems, it was postulated by Miller and Trauner that the biosynthesis of 9,10-deoxytridachione (**8**) and photodeoxytridachione (**11**) may occur from the same polyene precursor **30** *via* two different cyclisation processes, as depicted in Scheme 1.5.[23,24]

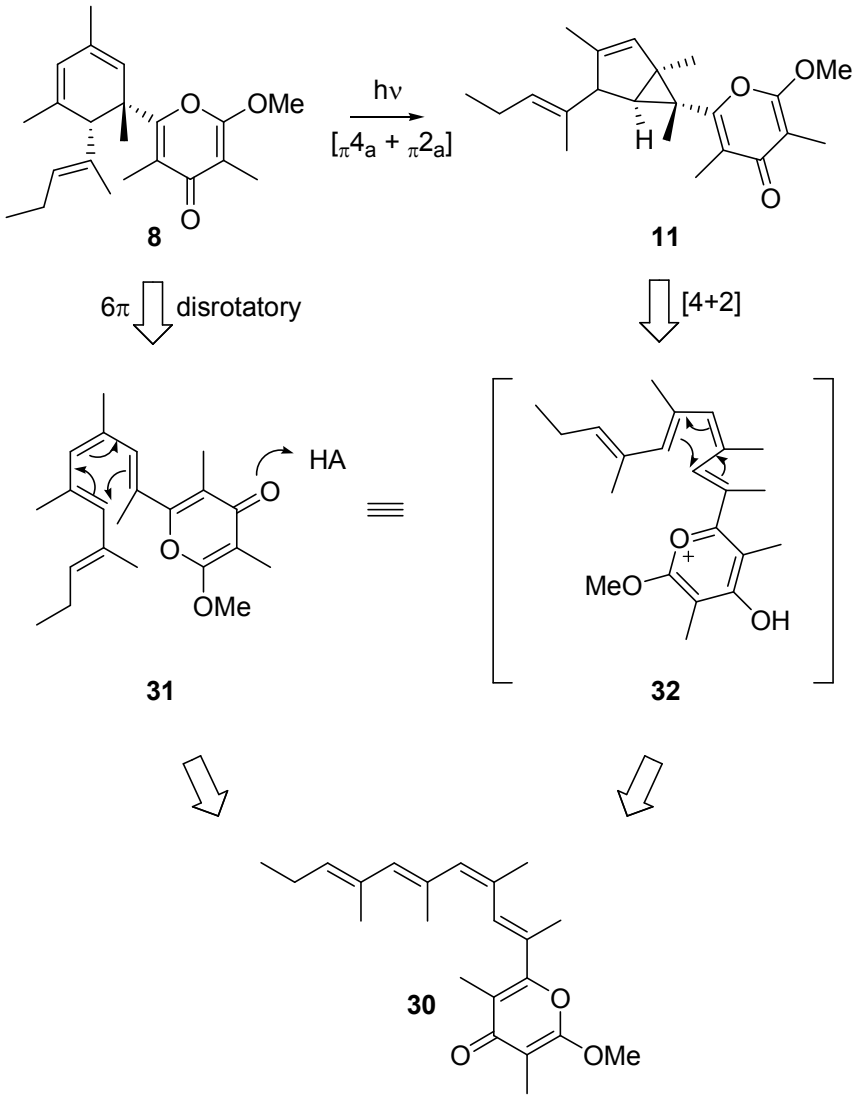

*Scheme 1.5. The proposed cyclisation processes involved in the formation of **8** and **11** from a common precursor **30**.*

According to Scheme 1.5 a 6π disrotatory electrocyclisation of precursor **31** would produce cyclohexadiene **8**. In contrast, pyrylium ion **32** would arise as a result of protonation of **30** and, acting as an electron sink corresponding to the Lewis acid-activated ester **25** (Scheme 1.3) would cyclise *via* a [4+2] cycloaddition to produce photodeoxytridachione (**11**).

γ-Pyrone-containing polyene precursor **30** was utilised by Miller and Trauner in the synthesis of ocellapyrone A (**33**) (Scheme 1.6).[25,24]

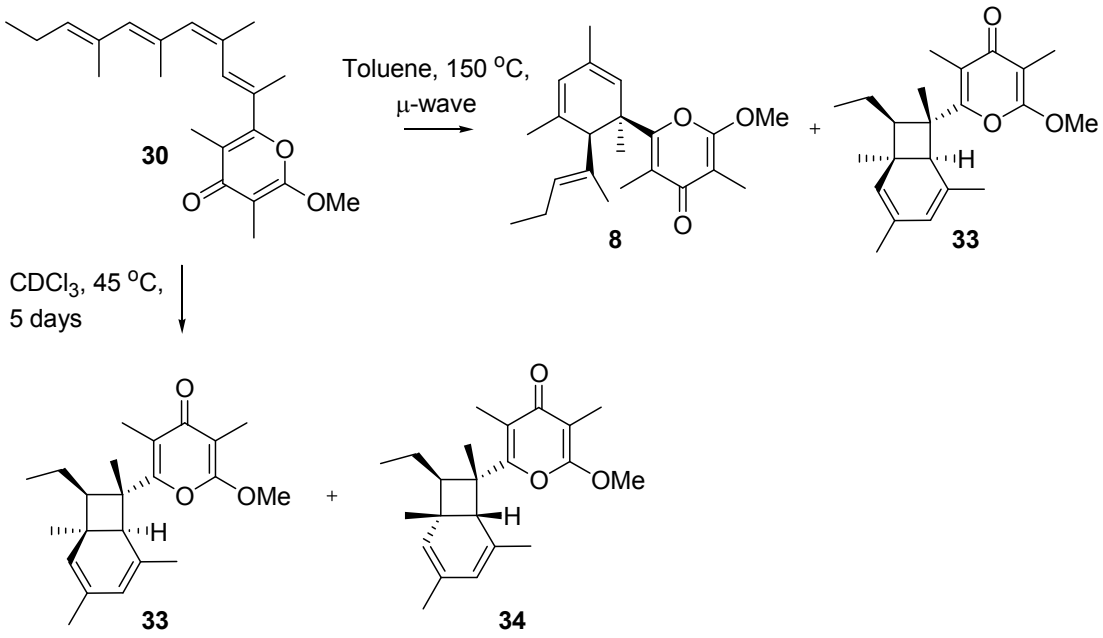

Scheme 1.6. Compounds isolated from reactions of γ-pyrone-containing tetraene ***30***.[25,24]

Exposure of polyene **30** to the two different reaction conditions described in Scheme 1.6 led to two different product profiles. Heating a solution of **30** in toluene to 150 °C in a microwave led to the formation of (±)-9,10-deoxytridachione (**8**) and ocellapyrone A (**33**), while warming of polyene **30** to 45 °C in $CDCl_3$ for 5 days led to formation of ocellapyrone A (**33**) and its diastereomer **34**. The results of this experiment provided further evidence for the biosynthesis of γ-pyrone-containing natural products from polyene precursors.

The hypothesis that both 9,10-deoxytridachione (**8**) and photodeoxytridachione (**11**) originate from the same precursor was also investigated by Moses *et al*.[23-25] In studies towards the biomimetic synthesis of crispatene (**16**), polyene **35** was converted to bicyclohexene **36** in the presence of sunlight (Scheme 1.7).[19]

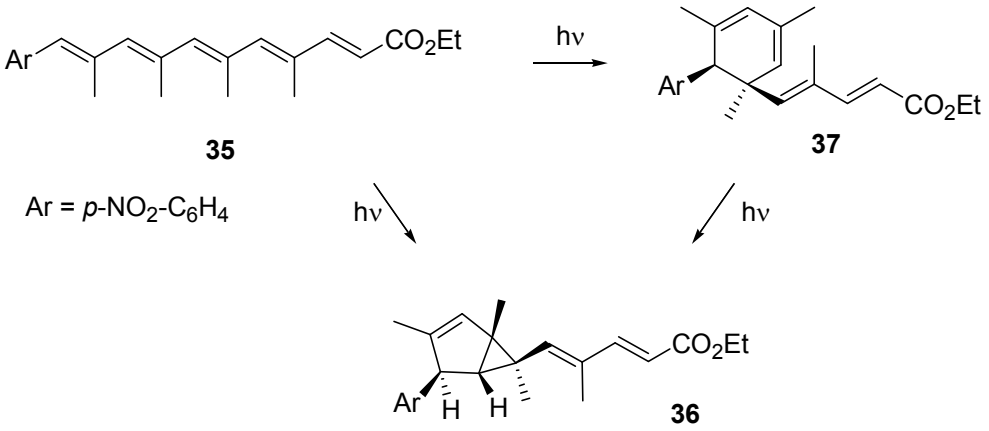

*Scheme 1.7. Formation of bicyclohexene **36** from polyene **35**.*[19]

Notably, a small amount of cyclohexadiene **37** was also isolated (Scheme 1.7), and it was subsequently found that **37** converted to bicyclohexene **36** upon standing in sunlight. It was also found that polyene **35** was not isolated at any stage during the conversion of cyclohexadiene **37** to bicyclohexene **36**. On this basis, it was concluded that the biosynthesis of photodeoxytridachione (**11**) may occur directly from 9,10-deoxytridachione (**8**), rather than through two different cyclisation processes from the one polyene precursor, as postulated by Miller and Trauner (Scheme 1.5).[23,24]

The synthesis of cyclohexadiene **37** from polyene **35** (Scheme 1.7) prompted investigations into the synthesis of 9,10-deoxytridachione (**8**) from a polyene precursor. To this end, a biomimetic synthesis of (±)-**8** was achieved from polyene **38** *via* a coupling of vinyl iodide **39** with boronic ester **40** (Scheme 1.8).[21]

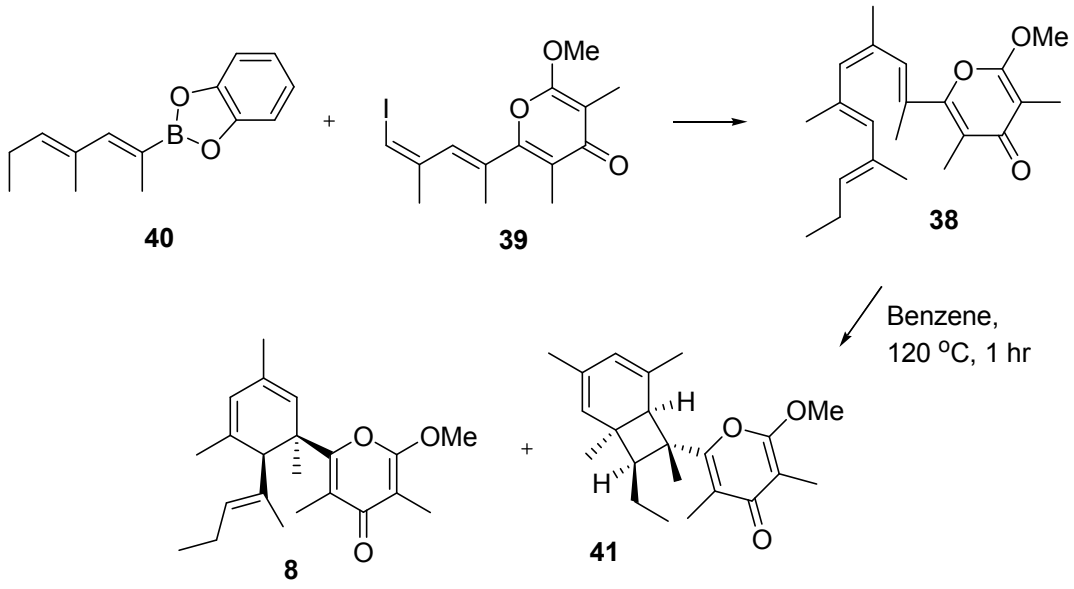

*Scheme 1.8. Synthesis of (±)-9,10-deoxytridachione (**8**) from polyene **38**.*[21]

The γ-pyrone-containing **41** was also isolated from this reaction (Scheme 1.8), the bicyclo-octadiene core of which is present in the natural products SNF4435C (**19**) and D (**20**) (Scheme 1.2). Thus, the biomimetic relationship between polyene precursors and tridachiapyrones was once again demonstrated.

From the studies described above, the link between the biosynthesis of polyene precursors and the presence of γ-pyrone-containing natural products in molluscs is strongly supported. Mimicking this mode of biosynthesis, the preparation of a number of tridachiapyrones, including (±)-9,10-deoxytridachione (**8**), was successfully carried out in a laboratory setting from a variety of polyene precursors. Another member of the γ-pyrone-containing polypropionate family, tridachiahydropyrone (reported as **14**, Figure 1.6),[17] has also been the subject of a number of synthetic studies, and these will be discussed in the following section.

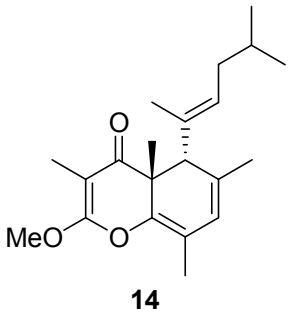

14

*Figure 1.6. Reported structure of tridachiahydropyrone (**14**).*

1.3.2 Studies towards tridachiahydropyrone (14)

Tridachiahydropyrone (**14**) was isolated from *Elysia crispata* off the coast of Venezuela in 1996 by Gavagnin and co-workers.[17] The biomimetic synthesis of tridachiahydropyrone (**14**) has not been as extensively investigated as that of 9,10-deoxytridachione (**8**). However, interest in this compound has recently evolved, due to discrepancies in the reported stereochemical relationship between the two adjacent stereocentres.

The structure of tridachiahydropyrone (**14**) was reported as that given in Figure 1.6 above with *anti* stereochemistry between the quaternary stereocentre bearing the methyl group, and the adjacent stereocentre bearing the alkene side-chain.[17] This stereochemical assignment was based on the observation of a Nuclear Overhauser Effect Spectroscopy (NOESY) correlation between the proton on C9 and the methyl protons on C17 (Figure 1.7).

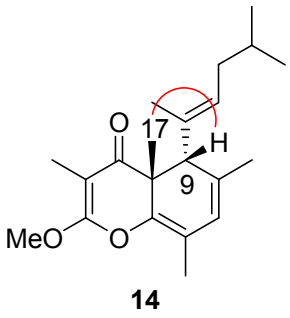

14

Figure 1.7. NOESY correlation observed between H9 and the protons of C17.

Synthesis of *anti* tridachiahydropyrone (**14**) (Figure 1.7) was undertaken in the Perkins group by David Jeffery,[26] and will be discussed in detail in Section 1.5. The stereochemistry of key intermediates *en route* to **14** was elucidated by both NOESY and X-ray crystallography, confirming that the desired *anti* stereochemistry had been achieved. However, when the Nuclear Magnetic Resonance (NMR) data of *anti* tridachiahydropyrone (**14**) was compared with the data reported for the natural product, a number of discrepancies were observed, indicating that **14** was not the true structure of tridachiahydropyrone. Most of the inconsistencies between the two sets of data occurred in the region highlighted in Figure 1.8(a), and it has been proposed that the stereochemistry in the natural product may therefore be *syn*, as depicted by **42**.

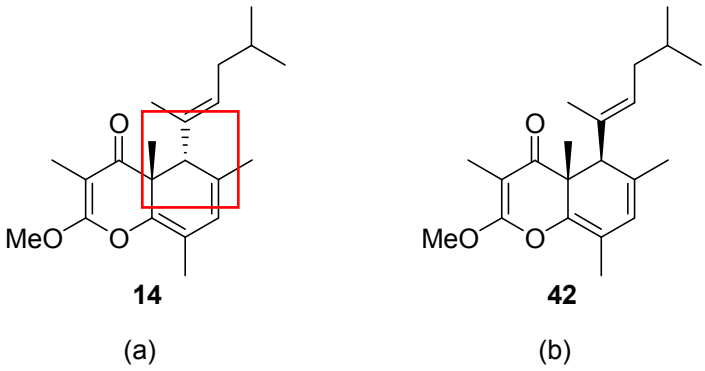

*Figure 1.8. (a) Region where inconsistencies were observed in the NMR data between anti tridachiahydropyrone (**14**) and the natural product. (b) Proposed true structure of tridachiahydropyrone.*

The *syn* relationship between the two adjacent stereocentres as depicted in *syn* tridachiahydropyrone (**42**) (Figure 1.8), was also identified in an α-pyrone-containing bi-cycle synthesised by Zuidema and Jones.[27] The study focussed predominantly on the photosensitisation abilities of a number of γ- and α-pyrone analogues, and it was found that α-pyrone **43** converted to *syn* bi-cycle **44** in the presence of UV light, when either benzene or piperylene was used as the solvent (Scheme 1.9).

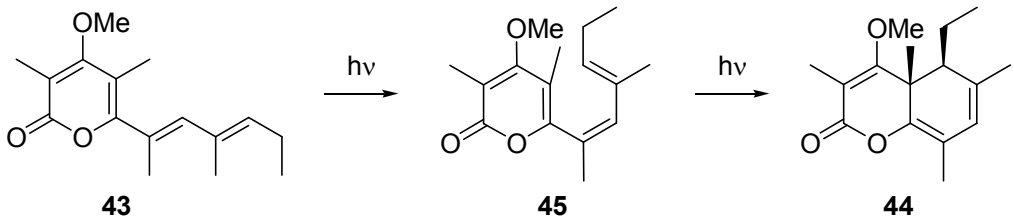

43 **45** **44**

*Scheme 1.9. Formation of syn α-pyrone **44** from diene **43**.*

This may therefore be another example of a biosynthesis of a pyrone-containing polypropionate from a polyene precursor in molluscs, and also lends weight to the hypothesis that the stereochemistry in tridachiahydropyrone may indeed be *syn*.

The synthetic endeavours described in Sections 1.3.1 and 1.3.2 towards 9,10-deoxytridachione (**8**) and tridachiahydropyrone (**14**) have opened the door to further studies into these interesting polypropionates. An enantiomerically-pure sample of 9,10-deoxytridachione (**8**) has not been prepared and the true structure of tridachiahydropyrone remains to be solved. The synthesis of 9,10-deoxytridachione (**8**) and *syn* tridachiahydropyrone (**42**) would allow their NMR and optical rotation data to be compared with that reported for the natural products, thus allowing the true structure and absolute stereochemistry of **8** and tridachiahydropyrone to be deduced.

The close relationship between the biosynthetic origins of tridachiapyrones **8** and **14** hints at the possibility of developing a common synthetic route to these two natural products. The potential exists of applying the synthetic methodology developed in the synthesis of *anti* tridachiahydropyrone (**14**),[26] to the preparation of both *syn* diastereomer **42** and 9,10-deoxytridachione (**8**). To this end, the work described herein will focus on synthetic efforts towards the preparation of *syn* tridachiahydropyrone (**42**) and 9,10-deoxytridachione (**8**).

There are two concepts, which are central to the understanding of the laboratory synthesis of polypropionates: the Felkin-Anh model of nucleophilic addition and the aldol reaction. These concepts will be discussed in the following section.

1.4 Concepts in the synthesis of polypropionates

1.4.1 Felkin-Anh model

The factors that affect the approach of nucleophiles to double bonds, particularly carbonyls, have been of significant interest to organic chemists. A number of models have been developed in order to understand the π-facial selectivity of kinetically-controlled nucleophilic addition to these functional groups, and currently the most widely-accepted model is the Felkin-Anh model.[28,29] This hypothesis predicts the direction of nucleophile approach to either aldehydes or acyclic ketones, which possess a stereogenic centre α to the carbonyl group.

The original model was based on the postulate by Felkin and Anh[28,29] that the torsional strain (known as the Pitzer strain, which occurs when bonds are eclipsed) "involving partially formed bonds represents a substantial fraction of the strain between fully formed bonds, even when the degree of bonding in the transition state is quite low".[28] The implication of this hypothesis is that the bonds of the transition state must be staggered, and has led to a model of nucleophile approach as depicted by rotamer **46** (**rot-46**) in Scheme 1.10, where the bulkiest of the α ligands (L) takes a position that is both perpendicular to the plane of the carbonyl group and *anti* to the incoming nucleophile (Nu). The next most sterically demanding α ligand (M) is placed gauche to the plane of the carbonyl group, giving a model of nucleophile (Nu) approach as shown in **rot-46** (Scheme 1.10).

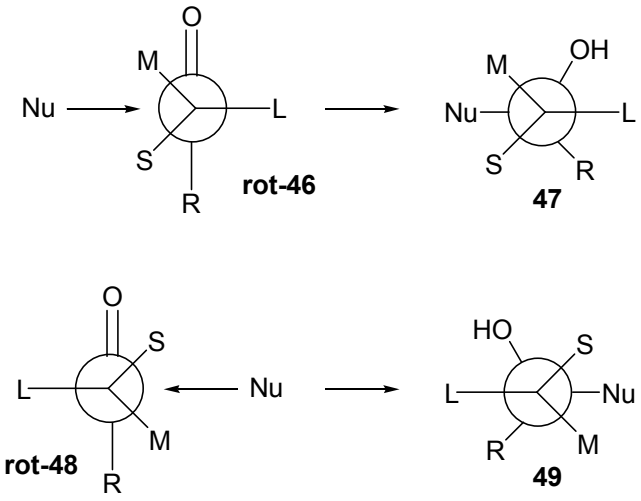

Scheme 1.10. The Felkin-Anh model of nucleophile addition to carbonyl groups.[28,29]

When R is small (e.g. a proton), **rot-46** and **rot-48** are almost energetically equivalent and hence it would be expected that **47** and **49** form in approximately a 1:1 ratio. However, as the size of R increases, the hindrance between the M and R groups in **rot-48** would cause **rot-48** (and the subsequent transition state) to be higher in energy. Thus, **rot-46** would be favoured, leading to an increase in the ratio of **47**:**49**. Evidence to support this hypothesis was given by the products of the reduction of phenyl ketones of type **50** by $LiAlH_4$ (Scheme 1.11), which gave predominantly the product of Felkin attack (**51**) in ratios (**51**/**52**) ranging from 2.8 (when R = Me) to 49 (when R = *t*-Bu).[28]

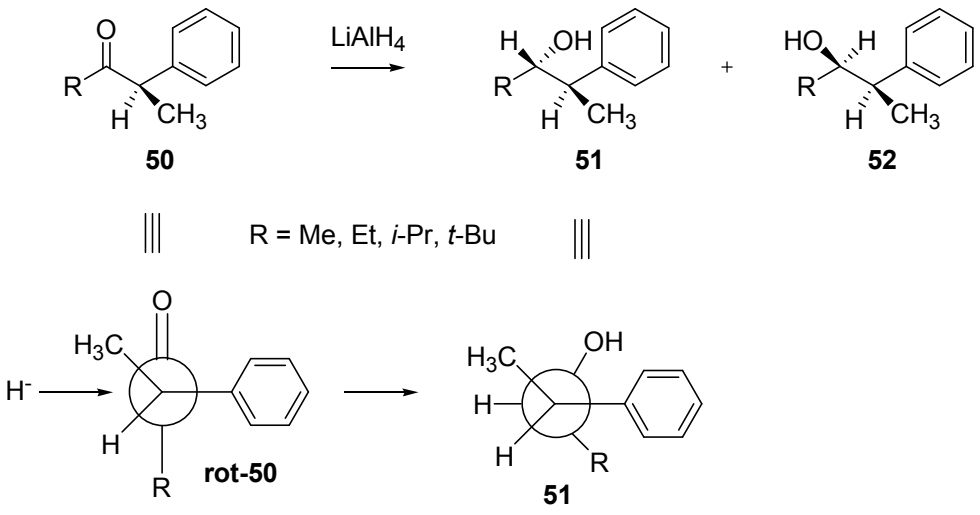

*Scheme 1.11. Reduction of phenyl ketone **50** exhibiting Felkin-Anh selectivity.*

Thus, the diastereoselectivity of nucleophilic addition increases (in most cases) as the size of R increases. Further, the Bürgi-Dunitz trajectory has refined the Felkin-Anh model.[30,31] In the Bürgi-Dunitz model, approach of the nucleophile occurs at an angle of approximately 109° to the plane of the carbonyl, making **rot-46** and **rot-48** energetically equivalent, regardless of the size of R (Figure 1.9). Therefore, nucleophile approach is dependent only on the steric interactions between the nucleophile and the ligands α to the carbonyl group.

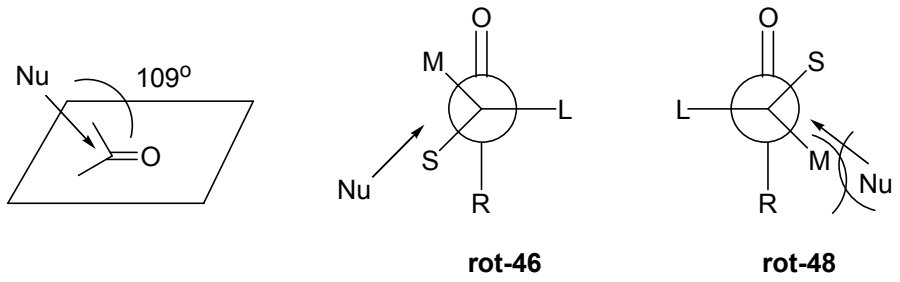

Figure 1.9. Bürgi-Dunitz angle stereoelectronic control.

Therefore, the transition state resulting from the approach of the nucleophile to **rot-46** (Figure 1.9) would be preferred over that of **rot-48**, due to the steric strain between the approaching nucleophile and ligand M in **rot-48**.

It can be seen from the preceding discussion that the Felkin-Anh[28,29] and Bürgi-Dunitz trajectory[30,31] models can be utilised to predict the approach of nucleophiles to carbonyl functionalities containing α-stereocentres, by taking into account the non-bonding interactions between the nucleophile and the ligands on the stereogenic centres. These models can also be applied to the addition of nucleophiles to α,β-unsaturated carbonyl systems.

In a study by Chounan *et al*[32] the facial preference of the addition of cuprates to *trans* and *cis* α,β-unsaturated esters was investigated. It was found that *trans* ester **53** produced *anti* product **54**, while *cis* ester **55** produced *syn* product **56** upon reaction with a variety of different cuprates (Scheme 1.12).

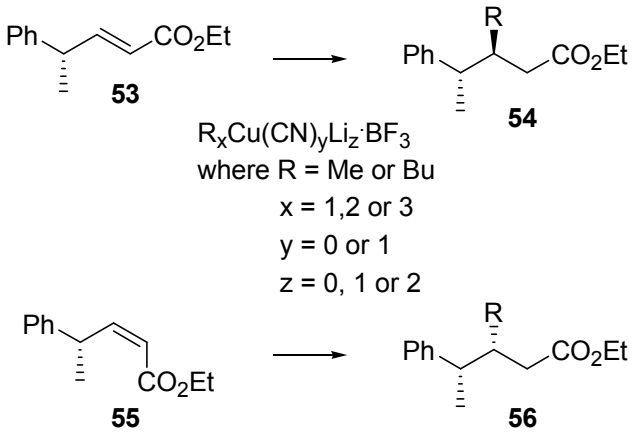

*Scheme 1.12. Stereochemical outcome of cuprate addition to esters **53** and **55**.*[32]

The ratio of **54**:**56** for *trans* ester **53** ranged from 80:20 (when $Bu_2CuLi{\cdot}BF_3$ was used) to 88:12 (when $BuCu{\cdot}BF_3$ was used), while the ratios for *cis* ester **55** ranged from 33:67 (when $Bu_2Cu(CN)Li_2{\cdot}BF_3$ was used) to 21:79 (when $Me_3CuLi_2{\cdot}BF_3$ was used).[32] The stereochemical outcome of these reactions (Scheme 1.12) was attributed to nucleophilic addition to esters **53** and **55** occurring *via* the Bürgi-Dunitz trajectory, as depicted in Scheme 1.13.

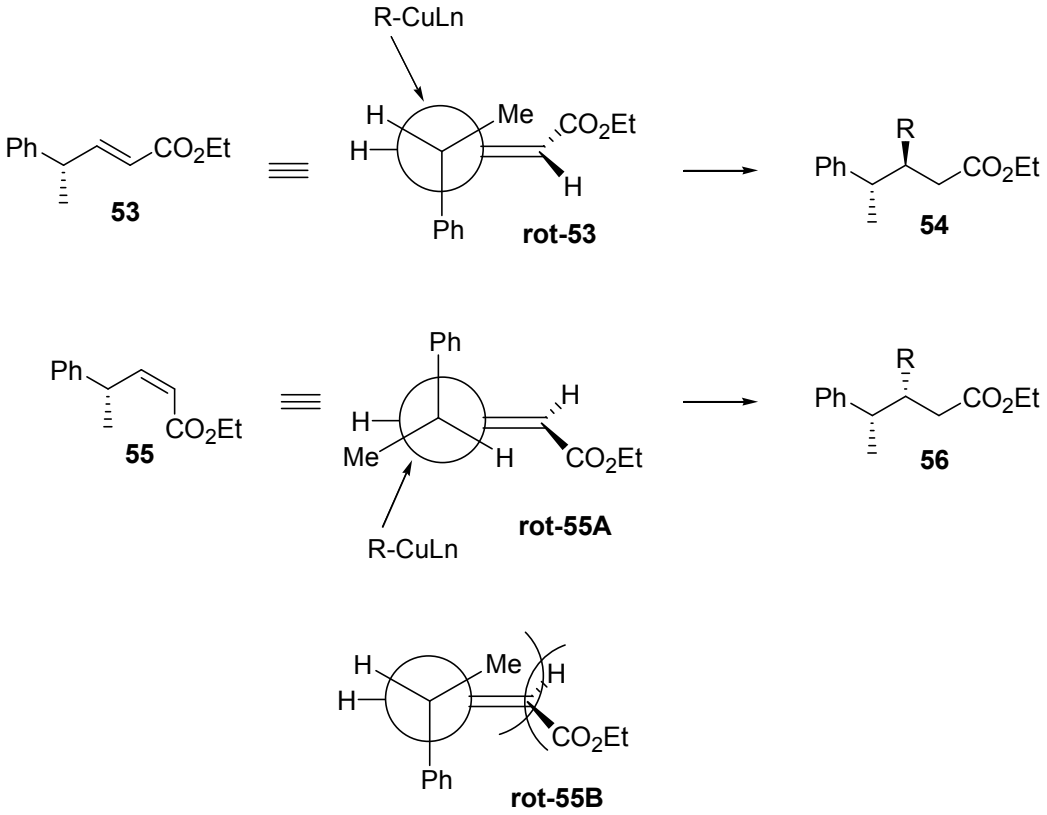

*Scheme 1.13. Bürgi-Dunitz trajectory model applied to the addition of cuprates to esters **53** and **55**.*[32]

In the case of *trans* ester **53** the favoured conformation was that depicted by **rot-53** (Scheme 1.13), where the phenyl group is perpendicular to the ester and the methyl group is gauche to the alkene. Approach of the nucleophile thus occurred *via* the predicted Felkin model, from outside of the rotamer (the least hindered position), to give the Felkin product **54**. In contrast, the same configuration of the rotamer of *cis* ester **55** would be de-stabilised due to the steric repulsion between the ester group and the methyl group (as shown in **rot-55B**). This resulted in **rot-55A** being more stable, as this minimised the allylic strain. The nucleophile then approached from the outside of **rot-55A** to give the observed *anti*-Felkin product **56**. The use of Felkin-Anh[28] and Bürgi-Dunitz trajectory[30,31] models to rationalise the outcome of nucleophile addition to both carbonyl groups and α,β-unsaturated carbonyl systems is an important concept in both the tandem conjugate addition-Dieckmann condensation reaction, which is a key step in the synthesis of *anti*

tridachiahydropyrone (**14**) and will be discussed in Section 1.5, as well as the aldol reaction, which is the subject of the following section.

1.4.2 The aldol reaction

Aldol reactions are currently the most widely employed reactions in the synthesis of polypropionates, and involve the coupling of a ketone of type **57** and an aldehyde of type **58**, either of which may be chiral or achiral to give an alcohol (**60**) (Scheme 1.14).

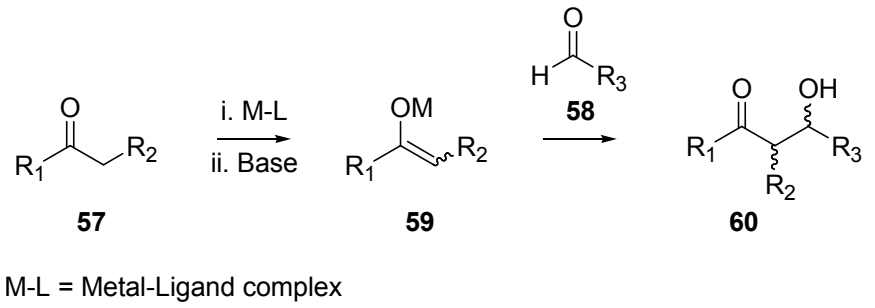

*Scheme 1.14. A general representation of an aldol reaction between a ketone of type **57** and an achiral aldehyde of type **58**.*

While in some cases the Felkin-Anh model[28] can be invoked to predict and rationalise the stereochemical outcome of aldol reactions, factors such as the type of enolate **59** formed from ketone **57**, the use of auxiliaries and the stereochemistry of ketone **57** and/or aldehyde **58**, can influence the stereochemistry of the product. Thus, by selectively altering these contributing factors, aldol reactions can be utilised to introduce specific stereochemistry into the products formed. The influence of each of these contributing factors will now be discussed.

1.4.2.1 Enolate geometry

Cis (*Z*) enolates are known to produce predominantly aldol products where the two generated stereocentres are *syn* while *trans* (*E*) enolates give rise to *anti* stereochemistry in the major product of the aldol reaction. Therefore, the stereochemical outcome of aldol reactions can be controlled by the use of enolates of

different geometry, and the type of enolate generated depends on the base used in the reaction. For example, ketone **61** (when R = Et) was found to form predominantly *E* enolate **62** (70:30 *E*:*Z*) when lithium diisopropylamine (LDA) was used as the base, while in the same system, the use of lithium hexamethyldisilylazide (LiHMDS) as the base led to formation of predominantly *Z* enolate **63** (34:66) (Scheme 1.15).[33]

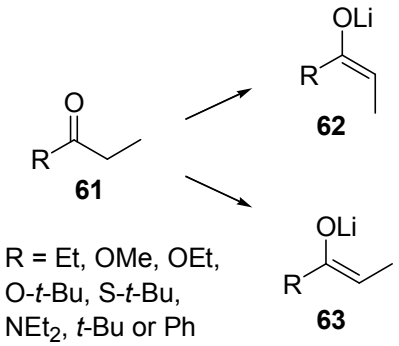

Scheme 1.15. E and Z lithium enolates, ***62*** *and* ***63****.*

As indicated in Scheme 1.15 a number of different ketones have been utilised in studies of the enolisation stereochemistry of lithium enolates. These studies involved reacting ketones of type **61** with different bases such as LDA, lithium tetramethylpiperidine (LTMP), LiHMDS and $(Bn_2N)_2SiLi$.[33-40] It was found that more sterically-demanding bases gave predominantly *E* enolate **62**, while an increase in the size of the R group led to formation of predominantly *Z* enolate **63**. Based on the results of these studies, Ireland *et al*[38] proposed a cyclic six-membered transition state to explain these observations (Scheme 1.16).

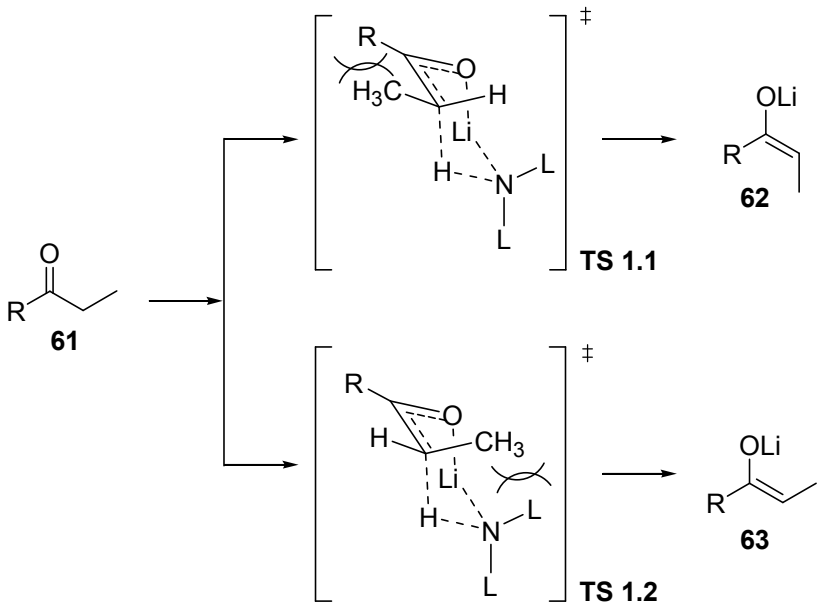

*Scheme 1.16. Proposed transition states **1.1** and **1.2** leading to formation of enolates **62** and **63**.*[38,41]

As depicted in Scheme 1.16, transition state (**TS**) **1.1** leading to *E* enolate **62** is disfavoured by the developing allylic strain between R and the methyl group of the enolate, while **TS 1.2** leading to *Z* enolate **63** is disfavoured by the 1,3-diaxial interaction between the ligands on the nitrogen and the methyl group. Thus, the model proposed by Ireland *et al*[38] correlates well with the experimental results observed in the studies described above, where it was found that more *E* enolate **62** was formed when the ligands on the base were large, while *Z* enolate **63** was favoured as the size of R increased.

Boron Lewis acids bearing either chiral or achiral ligands in combination with tertiary amine bases are also commonly used in the formation of enolates for aldol chemistry, as they are both versatile and effective.[41] A number of chiral boron Lewis acids, all of which give *Z* enolates, are pictured on the following page (Figure 1.10).[42,43]

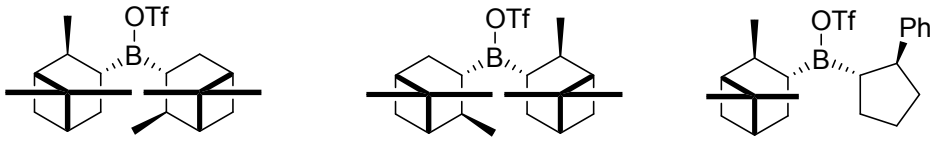

64 **65** **66**

Figure 1.10. Chiral boron Lewis acids utilised in aldol chemistry.

For the purpose of this discussion, however, the focus will be placed on the use of achiral boron Lewis acids. There are currently two major achiral ligands used in boron-mediated aldols, namely cyclohexyl (*c*-C_6H_{11}) [44-46] and *n*-Bu,[47] and either boron chlorides or triflates can be used. The type of enolate formed from either achiral boron chlorides or triflates can be rationalised using **TS 1.3** and **1.4**[41] depicted in Scheme 1.17.

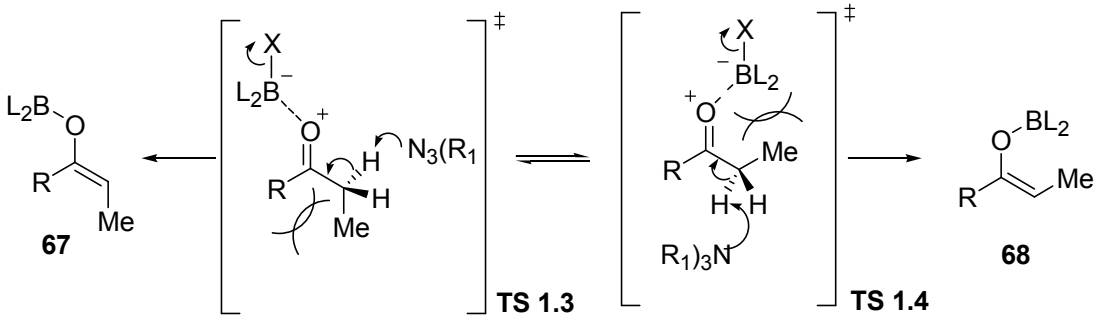

*Scheme 1.17. Steric interactions in enolate transition states **1.3** and **1.4** giving rise to the formation of enolates with different geometries **67** and **68**.*

The geometry of the enolate formed in each case (Scheme 1.17) can be rationalised by taking into account the steric interactions between the methyl of the enolate and either the R group of the enolate or the ligands (L) on the boron. Thus, larger ligands on the Lewis acid favour the formation of *E* enolate **67**, while the larger R group will favour the formation of *Z* enolate **68**. It has also been shown that boron triflates favour the formation of *Z* enolates, while chloride reagents favour *E* enolate geometry.[41] While these rules apply in the majority of cases, it should be noted that certain ketones may exhibit alternative preferences. However, in a practical sense

and in the majority of cases, a boron triflate with small ligands (eg *n*-Bu or Et) can be utilised to form selectively *Z* enolates, while a boron chloride with large ligands (eg *c*-C_6H_{11}) can be utilised to form *E* enolates selectively.

The geometry of the enolate can also be affected by the use of chiral auxiliaries, which can either be permanently incorporated into the framework of a molecule or selectively cleaved at a later stage in the synthesis. While the list of auxiliaries available to synthetic chemists is extensive, and includes, among others, compounds derived from ephedrine, carbohydrates and silicon,[41] the most widely-used auxiliaries in polyketide synthesis are the oxazolidinones **69** – **72** developed by Evans,[45,47-52] which are derived from amino acids (Figure 12).

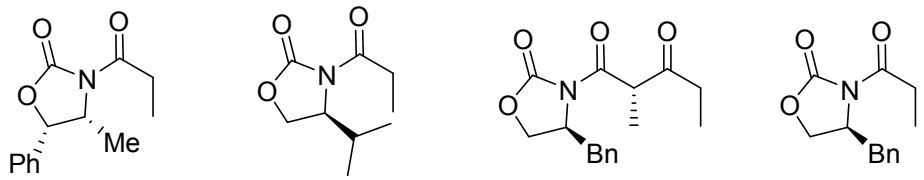

69 **70** **71** **72**

Figure 1.11. N-acyloxazolidinones utilised as chiral auxiliaries in stereoselective synthesis.

These auxiliaries are readily enolisable and have been shown to form predominantly *Z* enolates upon treatment with a base and a Lewis acid, which can be rationalised by taking into account **TS 1.3** and **TS 1.4** in Scheme 1.17 above. The aldol products formed from these chiral enolates are also almost exclusively *syn*, and as such, these auxiliaries are particularly useful in controlling the stereochemical outcome of aldol reactions. The most common oxazolidinone auxiliaries currently in use are **72** (Figure 1.11) and its enantiomer, as a result of their ease of synthesis from commercially available starting materials, namely the amino acids (*S*)- and (*R*)-phenylalanine.

From the above discussion it can be seen that factors which affect enolate geometry, such as the types of bases and Lewis acids utilised, as well as the use of chiral

auxiliaries to form chiral enolates, play a significant role in the stereochemical outcome of aldol reactions. While it has been mentioned in the above discussion that there is a link between enolate geometry and aldol stereochemistry, the reasons for this have not been considered. Commonly, the outcome of aldol reactions is rationalised through the use of Zimmerman-Traxler (Z-T) transition states, which will be discussed in the following section.

1.4.2.2 Zimmerman-Traxler transition states

The Z-T transition states are closed transition states in which the aldehyde carbonyl complexes to the Lews acid in a 6-membered transition state, and are a useful tool in helping to rationalise the stereochemistry of the major and minor products formed in aldol reactions. In the simplest case, where achiral aldehyde **58** is coupled to achiral ketone **57** *via* enolate **73**, the reaction ultimately leads to the introduction of two new stereocentres in the aldol product *via* the Z-T **TS 1.5** and **1.6** (Scheme 1.18).

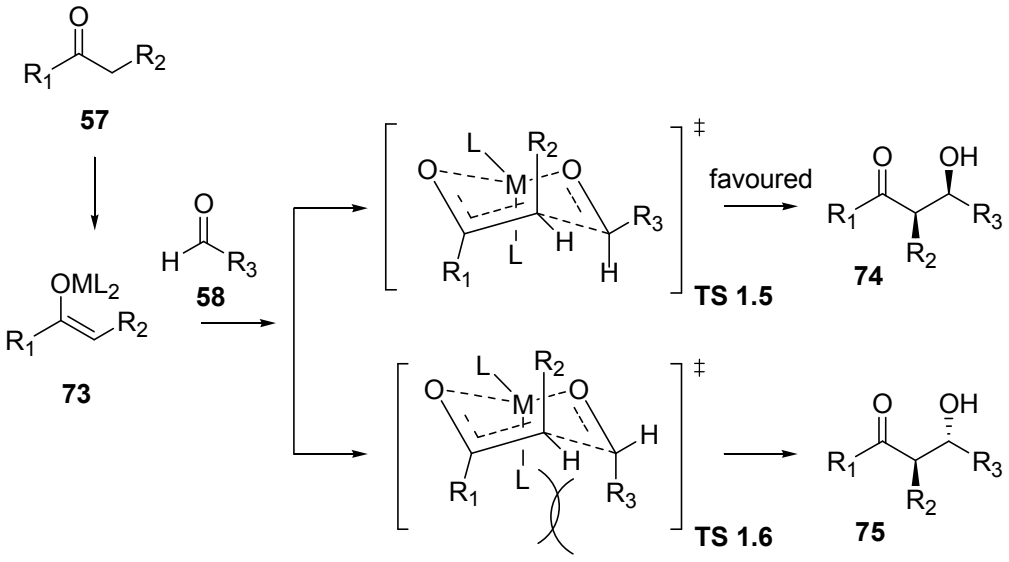

*Scheme 1.18. An aldol reaction between Z enolate **73** and achiral aldehyde **58**.*

Upon reaction of *Z* enolate **73** with achiral aldehyde **58**, two possible transition states (and their mirror images) can be formed (Scheme 1.18). The geometry about the double bond of enolate **73** is fixed and hence R_1 and R_2 are given as shown. However, R_3 can be either equatorial or axial. In the axial conformation (**TS 1.6**), there exists

steric strain between R_3 and R_1 and a 1,3-diaxial interaction between R_3 and the ligands (L) on the boron. Therefore **TS 1.6** is of a higher energy than **TS 1.5** and hence the favoured products are *syn* aldol products **74** and *ent*-**74**, derived from **TS 1.5**, and its mirror image.

A similar argument can be applied in the case of *E* enolate **76**, giving the products **77** and **78** as shown in Scheme 1.19, with **77** being the major product.

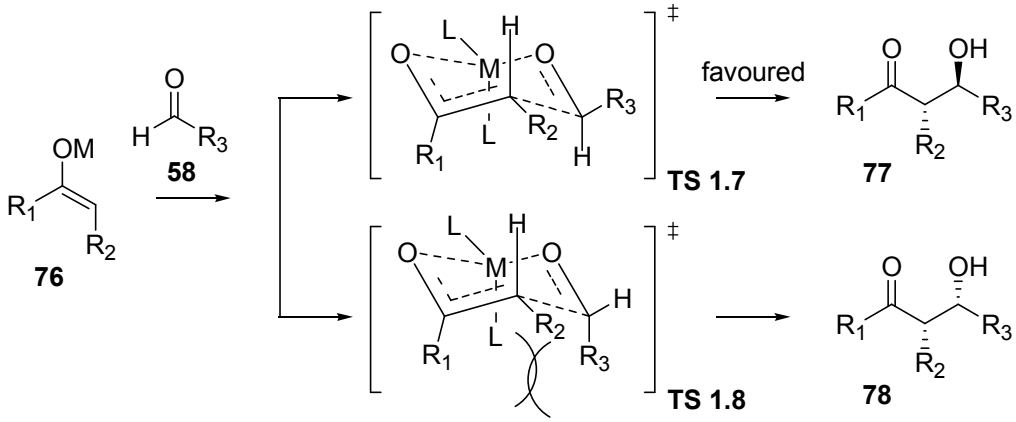

*Scheme 1.19. An aldol reaction between E enolate **76** and achiral aldehyde **58**.*

In the case of chiral auxiliaries such as **72** (Figure 1.11), the trend for formation of the *Z* enolate (as discussed previously in Section 1.4.2.1) leads to the formation of predominantly *syn* aldol products of type **79** (Scheme 1.20).

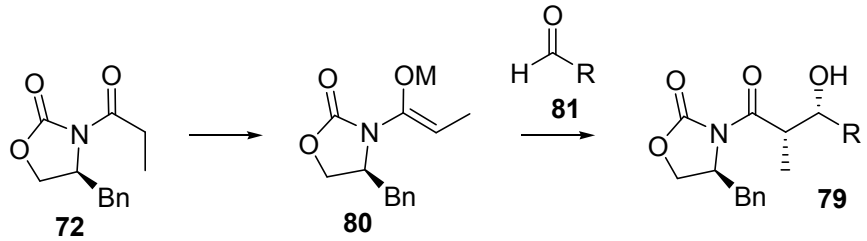

*Scheme 1.20. An aldol reaction between Z enolate **80** and achiral aldehyde **81**.*

Notably, the two new stereocentres are *anti* with respect to the stereocentre bearing the benzyl group of the oxazolidinone (Scheme 1.20). This can be attributed to the

preferred orientation of the C-N bond of the oxazolidinone in Z-T **TS 1.9** compared with **TS 1.10** (as depicted in Scheme 1.21).

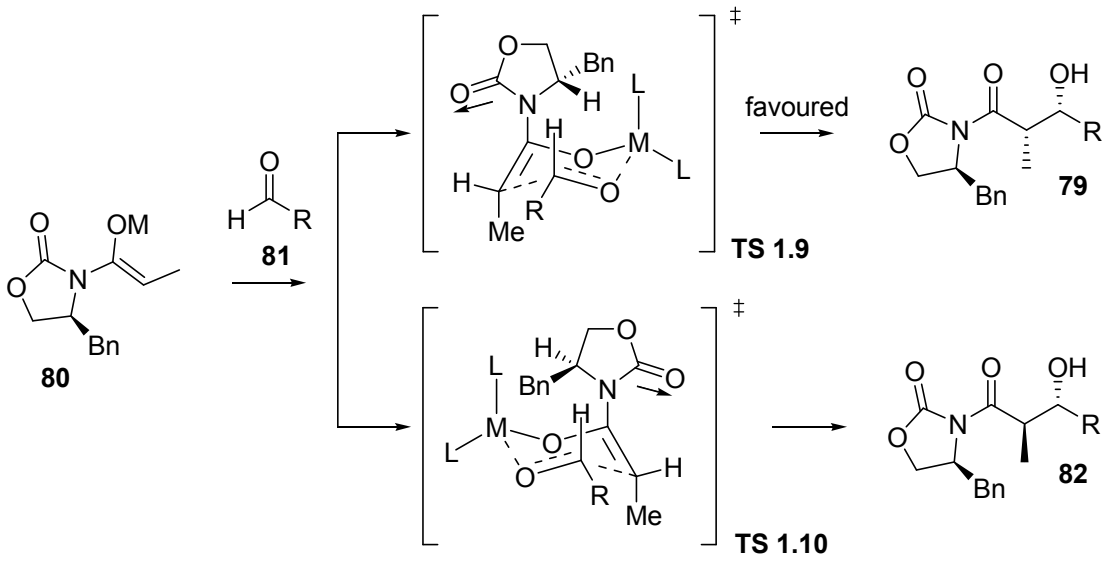

*Scheme 1.21. The preferred rotamer of the C-N bond in Z-T **TS 1.9** and **TS 1.10**.*

In both **TS 1.9** and **TS 1.10** (Scheme 1.21), the oxygen of the oxazolidinone is *anti* to the oxygens of the Z-T TS, as this orientation minimises electron repulsion. However, in **TS 1.9**, it is the proton, not the sterically-demanding Bn group (as in **TS 1.10**), which is positioned over the transition state. Thus, **TS 1.9** is favoured over **TS 1.10**, leading to the observed stereochemical outcome for the major product **79**.

It has also been shown in the case of aldehydes bearing an α-stereocentre, that the the auxiliary often overrides any facial preference the chiral aldehyde may have, producing *anti*-Felkin product **83** (with a ds greater than 95:5) from an aldehyde of type **84**[53,54] and Felkin product **85** from the enantiomer, aldehyde **86**[55*] (Scheme 1.22).

[*] The ds was not reported for aldol product **85** in this reference, as **85** was prepared from (±)-**86**.

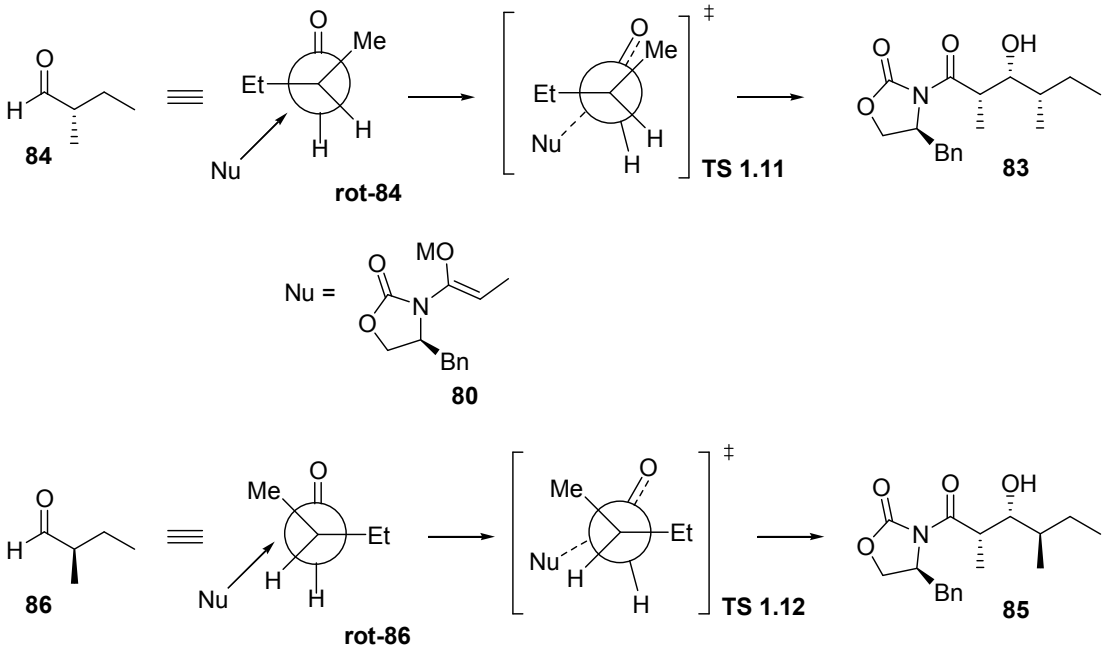

*Scheme 1.22. Anti-Felkin and Felkin addition of enolate **80** to aldehydes **84** and **86**.*[54-56]

Thus, overall, the outcome of aldol reactions can be controlled by varying factors such as the enolate geometry (through the use of different Lewis acids and ketones) and incorporating the use of auxiliaries. Additionally, various models, such as the Felkin-Anh[28] and Burgi-Dunitz trajectory[30,31] models and the Z-T transition states, can be used to rationalise and predict dominant nucleophilic addition and aldol products.

These concepts were central to the development of the synthesis of *anti* tridachiahydropyrone (**14**).[26] In the interest of utilising a synthetic methodology that could be applied to the preparation of a number of members of the tridachiapyrone family, it was envisaged that the synthetic methodology used for the synthesis of *anti* tridachiahydropyrone (**14**) could be further developed and applied to the synthesis of both 9,10-deoxytridachione (**8**) and *syn* tridachiahydropyrone (**42**). Therefore, it is now necessary to explain the synthetic approach towards *anti* tridachiahydropyrone (**14**). This will highlight a number of additional key concepts, which will be vital to understanding the synthetic approaches towards 9,10-deoxytridachione (**8**) and *syn* tridachiahydropyrone (**42**) discussed in subsequent chapters.

1.5 Synthesis of *anti* tridachiahydropyrone (14)

As mentioned previously in Section 1.3.2, the approach to *anti* tridachiahydropyrone (**14**) was developed in the Perkins group by a previous Ph.D. student.[26,56,57] The synthesis of **14** began with the coupling of Evans auxiliary **72** with aldehyde **87** (which was derived from the commercially-available (*S*)-Roche ester **88** to give *syn* aldol product **89** (Scheme 1.23).[26]

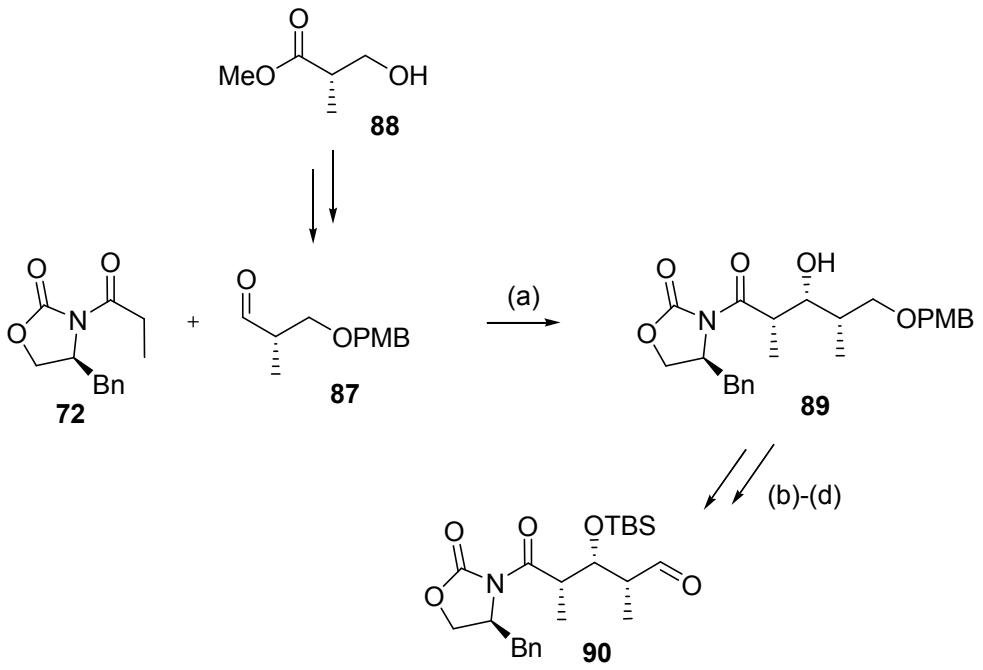

Reagents and conditions. (a) i. **72**, Bu_2BOTf, Et_3N, CH_2Cl_2, 0 °C. ii. **87**, – 78 °C → 0 °C, 83%; (b) TBSOTf, 2,6-lutidine, CH_2Cl_2, – 78 °C, 97%; (c) DDQ, pH 7 buffer, CH_2Cl_2, 0 °C, 96%; (d) DMSO, $(COCl)_2$, Et_3N, CH_2Cl_2, – 78 °C → 0 °C, 99%.

*Scheme 1.23. Synthesis of aldehyde **90** as an intermediate in the synthesis of anti tridachiahydropyrone (**14**).*

Syn aldol product **89** was then taken through to aldehyde **90** (Scheme 1.23), which was subsequently reacted with phosphonate **91** (derived from ester **88**) to give *trans* enone **92** (Scheme 1.24).

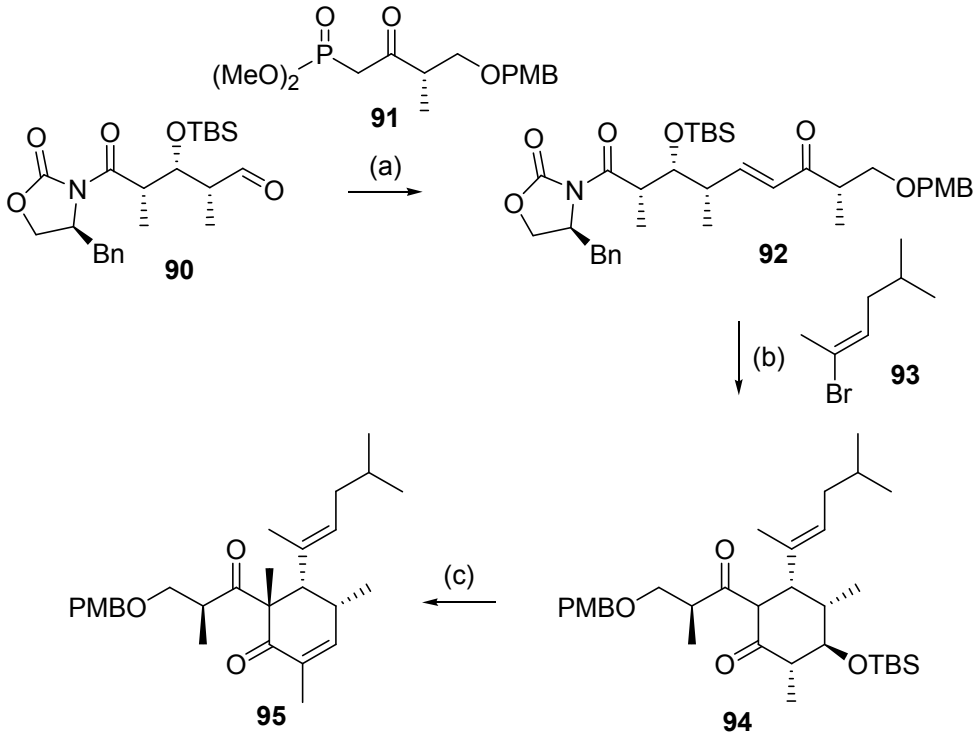

*Scheme 1.24. Synthesis of anti methylated cyclohexenone **95**.*

Reagents and conditions. (a) DIPEA, LiCl, MeCN, RT, 64%; (b) i. **93**, *t*-BuLi, THF, – 100 °C. ii. CuCN, Et_2O, – 78 °C → – 50 °C. iii. **92**, – 50 °C → 0 °C, 60%; (c) i. NaH, MeI, THF, RT. ii. NaH, RT, 77%.

The subsequent reaction of **92** with the dialkyl cuprate of bromoalkene **93** to give cyclohexanone **94** (Scheme 1.24) is a novel cyclisation method developed within the Perkins group for the synthesis of highly substituted chiral cyclohexanones.[56] Dialkyl cuprate **96** of bromoalkene **93** added to enone **92** in a 1,4-addition to give intermediate **97**, which underwent an intramolecular cyclisation producing cyclohexanone **94** and eliminating oxazolidinone **98** in the process (Scheme 1.25).

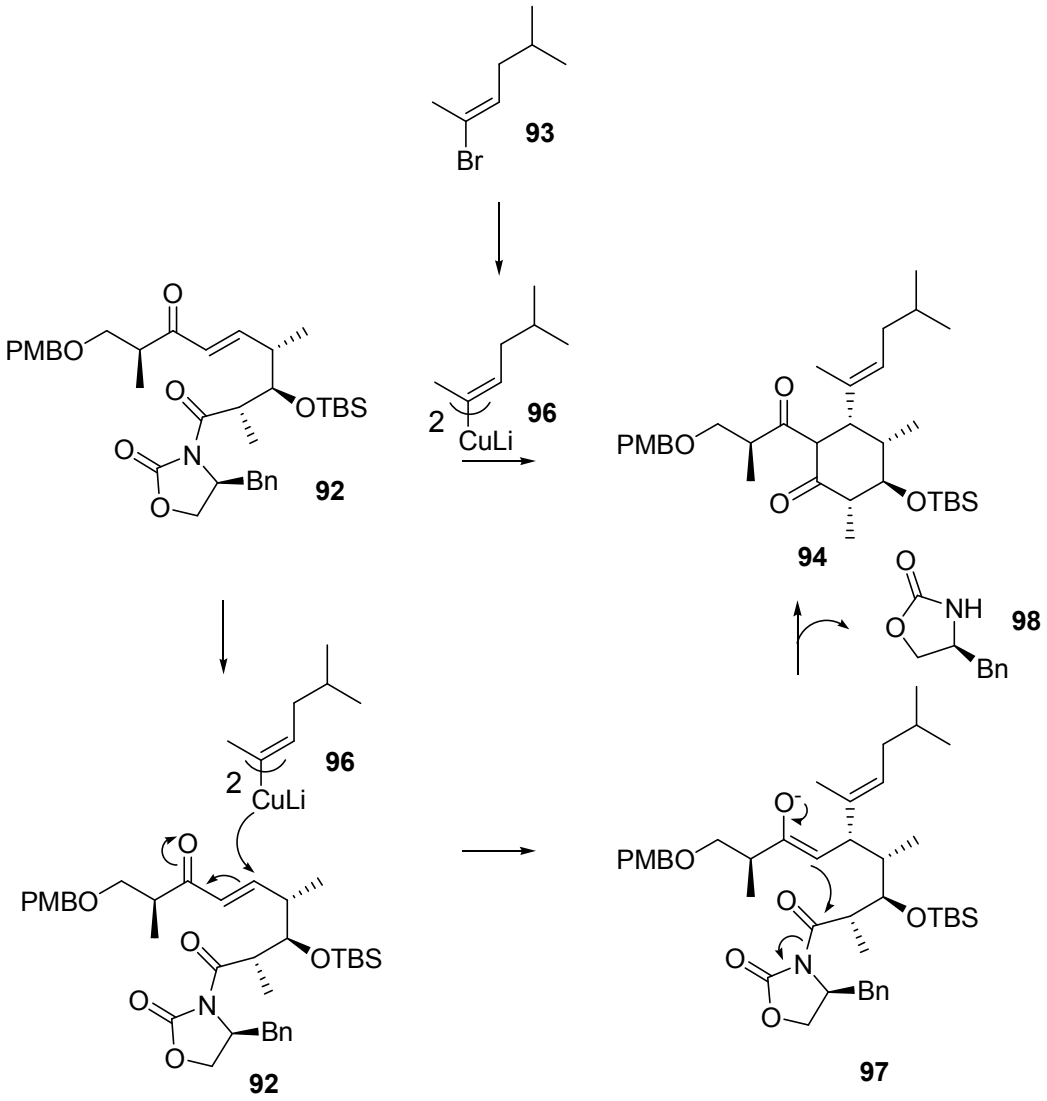

*Scheme 1.25. Addition of cuprate **96** to enone **92** producing cyclohexanone **94**.*

The stereochemical outcome of the cuprate addition depicted in Scheme 1.25 can be rationalised using a modified Felkin-Ahn model of nucleophile approach to α,β-unsaturated carbonyl compounds (Scheme 1.26).[28,32]

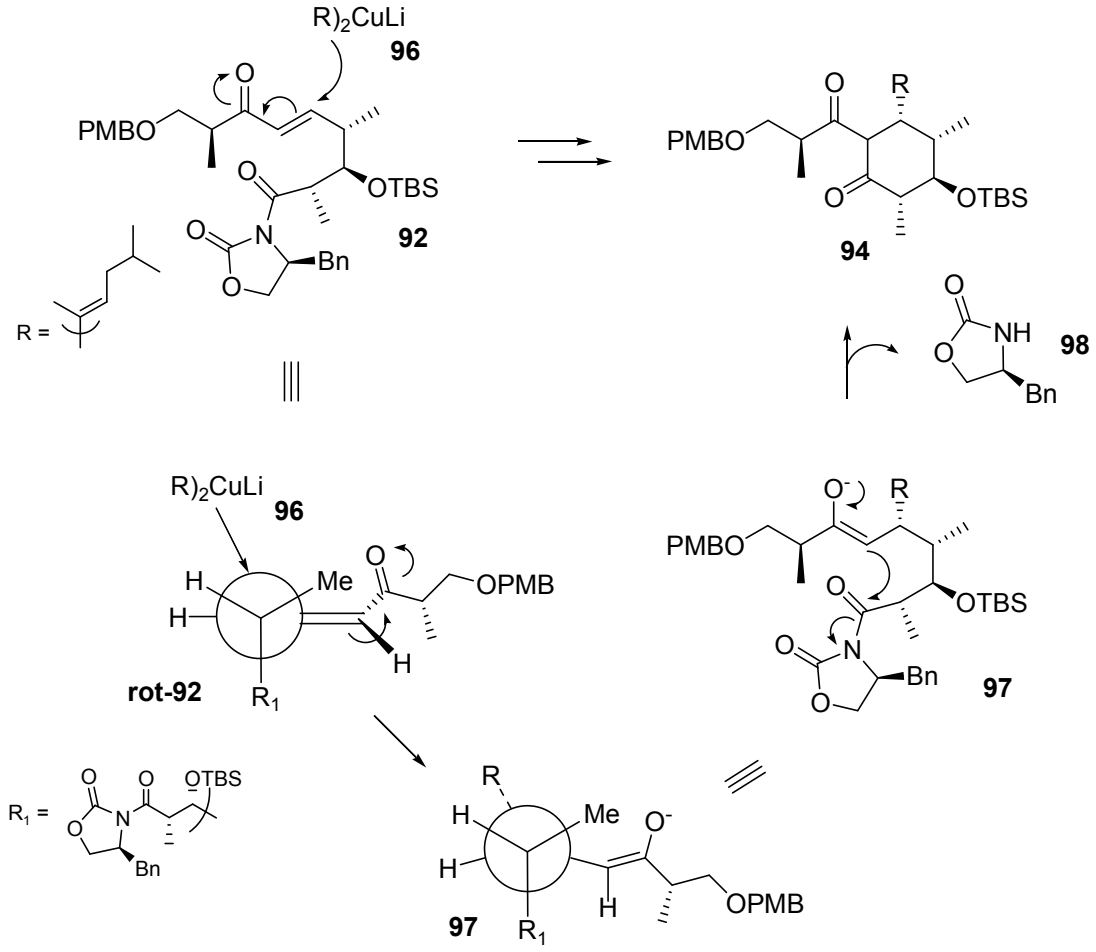

*Scheme 1.26. Modified Felkin-Anh model of nucleophile approach to enone **92**.*

The favoured rotamer of enone **92** was that depicted in Scheme 1.26, with R_1 perpendicular to the carbonyl and the methyl group inside the rotamer, as discussed in Section 1.4.1. The nucleophile (in this case cuprate **96**) approached the favoured rotamer of enone **92** from the least hindered position (as predicted by the Felkin-Anh model[28] and Chounan *et al*[32]) to give intermediate **97** (Scheme 1.26). Upon cyclisation, this produced the Felkin product, cyclohexanone **94**, with stereochemistry as depicted. The favoured chair conformation of cyclohexanone **94** was predicted to be that depicted in Scheme 1.27, with the alkene side-chain, affixed as a result of the cuprate addition, in the axial position and the other major groups in the equatorial position.

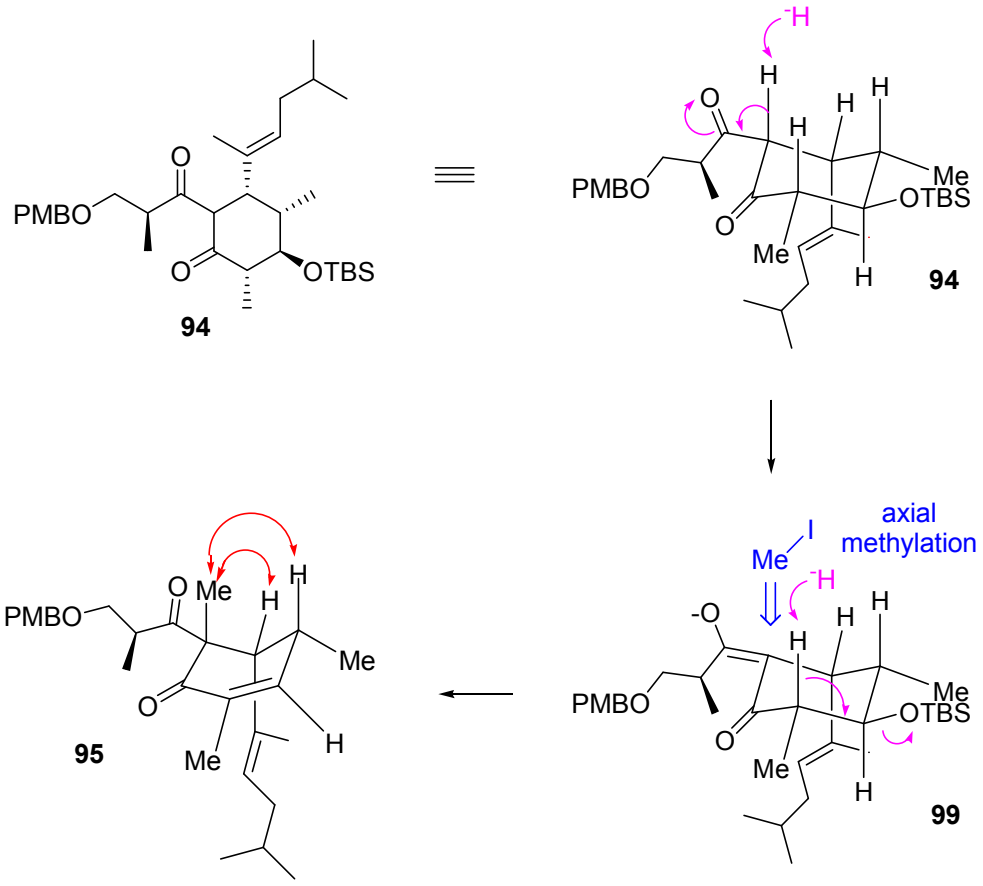

*Scheme 1.27. Conversion of cyclohexanone **94** to anti methylated cyclohexenone **95**.*

The stereochemistry in enone precursor **92** was chosen such that, upon cyclisation to give cyclohexanone **94**, all of the major groups would be in the equatorial position (as depicted in Scheme 1.27). It was believed that this would make the cyclisation thermodynamically-favourable, and hence drive the formation of **94**. Subsequent methylation of cyclohexanone **94** proceeded from the axial position as depicted in **99**, and, following elimination of the OTBS group, gave *anti* methylated cyclohexenone **95**. The *anti* stereochemistry between the quaternary methyl and alkene side-chain of **95** was verified by the presence of the NOESY correlations shown in Scheme 1.27.[57]

The synthesis of *anti* methylated cyclohexenone **95** allowed the required functional group manipulations to be undertaken, to give *anti* tridachiahydropyrone (**14**) and the α-pyrone analogue **100** (Scheme 1.28).

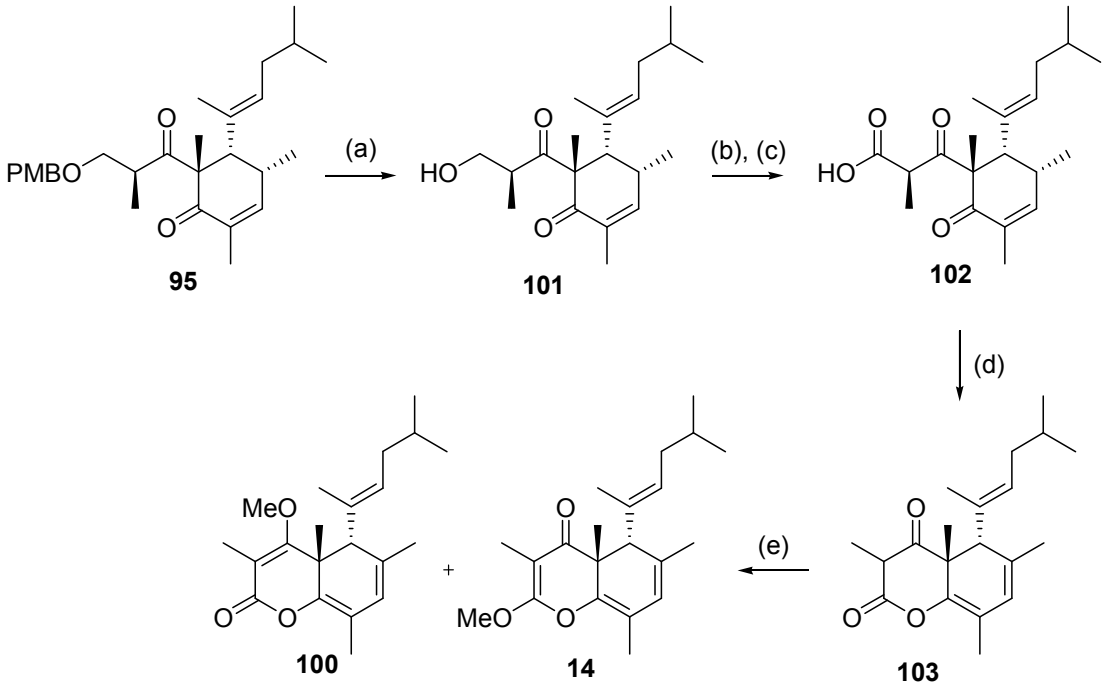

Reagents and conditions. (a) DDQ, pH 7 buffer, CH_2Cl_2, 0 ^oC, 93%; (b) DMP, CH_2Cl_2, RT, 100%; (c) $NaClO_2$, NaH_2PO_4, Me_2C=CHMe, *t*-BuOH, H_2O, RT, 88%; (d) P_2O_5-celite, CH_2Cl_2, RT, 56%; (e) CH_2N_2, Et_2O, RT, 45% **100** and 36% **14**.

*Scheme 1.28. Synthesis of anti tridachiahydropyrone (**14**) and α-pyrone analogue **100**.*

Cleavage of the PMB group from *anti* methylated cyclohexenone **95** gave alcohol **101**, which was a crystalline compound. An X-ray crystal structure of **100** was obtained, and confirmed the stereochemistry deduced previously by NOESY correlations (depicted in Scheme 1.27). Alcohol **101** was then taken through a two-step oxidation procedure to give acid **102**, which was subjected to dehydration conditions of P_2O_5 on celite, resulting in the formation of keto-ester **103**. Treatment of **103** with an excess of CH_2N_2 produced the two pyrones **14** and **100**, which were separable by column chromatography, in almost a 1:1 ratio (by mass). It was γ-pyrone **14** that was of interest in this case, as this was the reported structure of tridachiahydropyrone.[17] However, as discussed previously (Section 1.3.2) a comparison of the NMR data of *anti* tridachiahydropyrone (**14**) and the natural product indicated that the true structure of tridachiahydropyrone was not **14**. Compounds **104** and **105** with a *cis* alkene side-chain were also synthesised (Figure

1.12), but the NMR data of these compounds also did not match that reported for the natural product.[57]

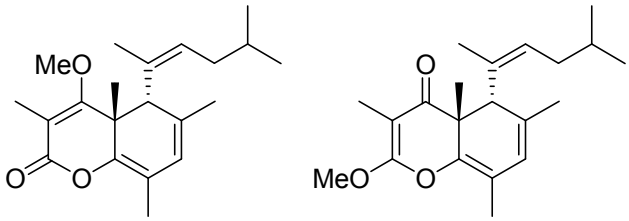

104 **105**

*Figure 1.12. Compounds **104** and **105**, with cis geometry of the alkene side-chain.*

It was thus proposed that the true structure of tridachiahydropyrone may be that depicted in **42** (Figure 1.13), where the two adjacent stereocentres are *syn*.

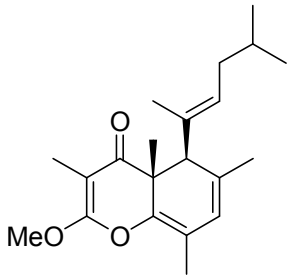

42

*Figure 1.13. Syn tridachiahydropyrone (**42**).*

1.6 Research aims

The puzzle of the true structure of tridachiahydropyrone made this an interesting synthetic target and also provided an avenue for extension of the methodology utilised in the synthesis of *anti* tridachiahydropyrone (**14**). The potential existed for using the novel tandem conjugate addition-Dieckmann condensation strategy to synthesise a number of stereochemically-diverse cyclohexanones. This would allow the scope and application of both the addition-cyclisation protocol and the subsequent methylation-elimination cascade to be tested. The ultimate aim was to synthesise *syn* tridachiahydropyrone (**42**) and extend the strategy to other members

of the tridachiapyrone family, namely the tethered analogue, 9,10-deoxytridachione (**8**) (Figure 1.14).

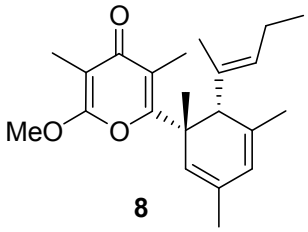

8

*Figure 1.14. 9,10-Deoxytridachione (**8**).*

The work described in the following chapters of this thesis focuses on synthetic endeavours towards both 9,10-deoxytridachione (**8**) and *syn* tridachiahydropyrone (**42**).

1.7 References

1. Blunden, G. *Phytother. Res.* **2001,** *15*, 89-94.
2. Davies-Coleman, M. T., Garson, M. J. *Nat. Prod. Rep.* **1998**, 477-93.
3. Hochlowski, J. E., Faulkner, D. J., Matsumoto, G. K., Clardy, J. *J. Am. Chem. Soc.* **1983,** *105*, 7413-5.
4. Hochlowski, J. E., Coll, J. C., Faulkner, D. J., Biskupiak, J. E., Ireland, C. M., Qi-tai, Z., Cun-heng, H., Clardy, J. *J. Am. Chem. Soc.* **1984,** *106*, 6748-50.
5. Gavagnin, M., Spinella, A., Castelluccio, F., Cimino, G. *J. Nat. Prod.* **1994,** *57*, 298-304.
6. Gavagnin, M., Marín, A., Mollo, E., Crispino, A., Villani, G., Cimino, G. *Com. Biochem. Physiol.* **1994,** *108B*, 107-15.
7. Ireland, C., Scheuer, P. J. *Science* **1979,** *205*, 922-3.
8. Cimino, G., Fontana, A., Gavagnin, M. *Curr. Org. Chem* **1999,** *3*, 327-72.
9. Marín, A., Ros, J. *Sci. Mar.* **2004,** *68 (Suppl. 1)*, 227-41.
10. Kato, S. (2002) http://www.seaslugforum.net/factsheet.cfm?base=volvviri
11. Chan, L. (2001) http://www.seaslugforum.net/factsheet.cfm?base=elyscfjapo
12. Imamoto, J. (2004) http://www.seaslugforum.net/factsheet.cfm?base=elysatro
13. Ireland, C., Faulkner, D. J., Solheim, B. A., Clardy, J. *J. Am. Chem. Soc.* **1978,** *100*, 1002-3.
14. Kay, P. S., Faulkner, D. J. *Bol. Soc. Chil. Quim.* **1984,** *29*, 329-32.
15. Dawe, R. D., Wright, J. L. C. *Tetrahedron Lett.* **1986,** *27*, 2559-62.
16. Ksebati, M. B., Schmitz, F. J. *J. Org. Chem.* **1985,** *50*, 5637-42.
17. Gavagnin, M., Mollo, E., Cimino, G. *Tetrahedron Lett.* **1996,** *37*, 4259-62.
18. Ireland, C., Faulkner, D. J. *Tetrahedron* **1981,** *37*, 233-40.
19. Moses, J. E., Baldwin, J. E., Brückner, S., Eade, S., Adlington, R. M. *Org. Bio. Chem.* **2003,** *1*, 3670-84.
20. Brückner, S., Baldwin, J. E., Moses, J., Adlington, R. M., Cowley, A. R. *Tetrahedron Lett.* **2003,** *44*, 7471-3.
21. Moses, J. E., Adlington, R. M., Rodriguez, R., Eade, S. J., Baldwin, J. E. *Chem. Com.* **2005**, 1687-9.
22. Beaudry, C. M., Trauner, D. *Org. Lett.* **2002,** *4*, 2221-4.
23. Miller, A. K., Trauner, D. *Angew. Chem.* **2003,** *42*, 549-52.

24. Miller, A. K., Trauner, D. *Synlett* **2006,** *14*, 2295-316.
25. Miller, A. K., Trauner, D. *Angew. Chem. Int. Edit.* **2005,** *44*, 4602-6.
26. Jeffery, D. W., Perkins, M. V., White, J. M. *Org. Lett.* **2005,** *7*, 1581-4.
27. Zuidema, D. R., Jones, P. B. *J. Phot. Photbi. Bio.* **2006,** *83*, 137-45.
28. Chérest, M., Felkin, H., Prudent, N. *Tetrahedron Lett.* **1968**, 2199-204.
29. Anh, N. T., Thanh, B. T. *New. J. Chem.* **1986,** *10*, 681-3.
30. Bürgi, H. B., Dunitz, J. D., Shefter, E. J. *J. Am. Chem. Soc.* **1973,** *95*, 5065-7.
31. Bürgi, H. B., Dunitz, J. D., Lehn, J. M., Wipff, G. *Tetrahedron* **1974,** *30*, 1563.
32. Chounan, Y., Ono, Y., Nishii, S., Kitahara, H., Ito, S., Yamamoto, Y. *Tetrahedron* **2000,** *56*, 2821-31.
33. Heathcock, C. H., Buse, C. T., Klieschick, W. A., Pirrung, M. C., Sohn, J. E., Lampe, J. *J. Org. Chem.* **1980,** *45*, 1066-81.
34. Fataftah, Z. A., Kopka, I. E., Rathke, M. W. *J. Am. Chem. Soc.* **1980,** *102*, 3959-50.
35. Masamune, S., Ellingboe, J. W., Choy, W. *J. Am. Chem. Soc.* **1982,** *104*, 5526-8.
36. Ireland, R. E., Wipf, P., Armstrong III, J. D. *J. Org. Chem.* **1991,** *56*, 650-7.
37. Ireland, R. E., Mueller, R. H. *J. Am. Chem. Soc.* **1972,** *94*, 5897-8.
38. Ireland, R. E., Mueller, R. H., Willard, A. K. *J. Am. Chem. Soc.* **1976,** *98*, 2868-77.
39. Evans, D. A., McGee, L. R. *Tetrahedron Lett.* **1980,** *21*, 3975-8.
40. Heathcock, C. H. In *Modern Synthetic Methods;* Scheffold, R. Ed.; Verlag Helvetica Chimica Acta: Basel, 1992; p. 1.
41. Rizzacasa, M., Perkins, M. *Stoichiometric Asymmetric Synthesis*, 1 ed.; Sheffield Academic Press: Sheffield, 2000.
42. Paterson, I., Lister, M. A. *Tetrahedron Lett.* **1988,** *29*, 585-8.
43. Paterson, I., Lister, M. A., McClure, C. K. *Tetrahedron Lett.* **1986,** *27*, 4787-90.
44. Paterson, I., Perkins, M. V. *J. Am. Chem. Soc.* **1993,** *115*, 1608-10.
45. Evans, D. A., Weber, A. E. *J. Am. Chem. Soc.* **1986,** *108*, 6757-61.
46. Paterson, I., Goodman, J. M., Isaka, M. *Tetrahedron Lett.* **1989,** *30*, 7121-4.
47. Evans, D. A., Kaldor, S. W., Jones, T. K., Clardy, J., Stout, T. J. *J. Am. Chem. Soc.* **1990,** *112*, 7001-31.

48. Evans, D. A., Ennis, M. D., Mathre, D. J. *J. Am. Chem. Soc.* **1982,** *104*, 1737-9.
49. Evans, D. A., Urpi, F., Somers, T. C., Clark, J. S., Bilodeau, M. T. *J. Am. Chem. Soc.* **1990,** *112*, 8215-6.
50. Evans, D. A., Clark, J. S., Metternich, R., Novack, V. J., Sheppard, G. S. *J. Am. Chem. Soc.* **1990,** *112*, 866-8.
51. Evans, D. A., Ng, H. P., Rieger, D. L. *J. Am. Chem. Soc.* **1993,** *115*, 11446-59.
52. Evans, D. A., Kim, A. S. *Tetrahedron Lett.* **1997,** *38*, 53-6.
53. Dias, L. C., Meira, P. R. R. *Tetrahedron Lett.* **2002,** *43*, 185-7.
54. Dias, L. C., Meira, P. R. R. *J. Org. Chem.* **2006,** *70*, 4762-73.
55. Kinoshita, K., Khosla, C., Kane, D. E. *Helv .Chim. Acta.* **2003,** *86*, 3889-907.
56. Jeffery, D. W., Perkins, M. V. *Tetrahedron Lett.* **2004,** *45*, 8667-71.
57. Jeffery, D. Ph.D., Flinders University, 2005.